Egy. J. Pure & Appl. Sci. 2023; 61(2):42-66

Egyptian Journal of Pure and Applied Science

Utilization of microbiome in biocontrol of some cancer cell line models: in vitro study

Nahed F. George [1], Saadia M. Essa [1], Aly Fahmy Mohamed [2], Samia Abdou Girgis [3]

[1] *Microbiology Department, Faculty of Science, Ain Shams University, Cairo, Egypt*
[2] *Former head of Research and Development sector, the holding company for production of vaccines, sera and drugs (EgyVac), Cairo, Egypt*
[3] *Clinical Pathology, Faculty of Medicine, Ain Shams University, Cairo, Egypt*

ARTICLE INFO

Received 12 May 2023
Accepted 28 July 2023

Keywords
Microbiome,
Secondary metabolites,
Anticancer compounds,
Cytotoxicity assay,
Pathological examination,
GCMS.

Correspondence
Nahed F. George

E-mail
Nahedfarid_P @sci.asu.edu.eg

ABSTRACT

The microbiome including fungi and bacteria secret biologically active secondary metabolites. Secondary metabolites have been recognized as a potential source of anticancer compounds. In this study, we reported the effect of some fungal and bacterial models secondary metabolites against human lung cancer cell line (A549), human hepatocellular carcinoma cell line (HepG2), and human breast adenocarcinoma cell line (MCF7). The evaluation of the anticancer effect is reported through cytotoxicity assay, which showed that viability and IC_{50} were concentration, cell type and metabolite dependent. Also, pathological examination showed variable effect on cellular content. GCMS report for the secondary metabolites for each microbiome. *Aspergillus fumigatus* and *Aspergillus flavus* were the most effective fungal strains in treatment of A549 cell line. *Aspergillus terreus* and *Aspergillus fumigatus* were the most effective fungal strains in treatment of HepG2 cell line. *Aspergillus terreus* and *Aspergillus flavus* were the most effective fungal strains in treatment of MCF7 cell line. *Bacillus paramycoides* was the most effective bacterial strain in treatment of A549, HepG2 and MCF7 cell lines. Histopathological changes detected under the effect of bacterial and fungal metabolites induced cellular and nuclear membrane irregularities, nuclear outlines and shrunken apoptotic bodies and peripheral chromatin condensation.

1. Introduction

The microbiome is the most important source for secondary metabolites. It has great medical application especially in the synthesis of anticancer compounds [1, 2].

For example, the diverse biological activity of *Penicillium janthinellum biourge* L asparaginase as reported by Saadia et al. [3]. Also, Saadia et al. [4] reported the antioxidant and antibacterial activity of *Teucrium Poliumi*.

Furthermore, Saadia et al. [5] also reported the biochemical studies on microbial L- Glutaminase and its applications. Saadia et al. [6] also, reported the characterization of white button mushroom and its biomedical applications. Anticancer agents may be derived from secondary metabolites [7, 8]. Intriguing findings from recent studies were previously reported by Chakrabhavi et al. [9] and Saadia et al. [10] that imply bacteria can be beneficial agents for cancer treatment. The development of a new generation of cancer treatment medicines based on enzymes/proteins originating from microbes marked the beginning of a new era in cancer therapeutics. Yi et al. [11] came to this conclusion. These natural compounds general, and anticancer in particular will be used as a biological control against many different cancer diseases [2, 12]. Endophytes could be exploited for isolation of bioactive secondary metabolites as they provide molecules with unique structure [13].

In this study human lung cancer cell lines, human hepatocellular carcinoma cell lines and human breast adenocarcinoma cell lines are treated with *Aspergillus fumigatus*, *Aspergillus flavus, Aspergillus terreus* and *Penicillium sp. Voucher AC11* as fungal strains (humane microbiome and may be found in infected soil) as reported by Saadia et al. [14, 15], in addition to *Enterobacter cancerogenus*, *Bacillus subtilis spizizenii* and *Bacillus paramycoides (NR_157734.1)* as bacterial strains (humane microbiome and may be found in infected soil) as reported by Saadia et al. [16, 17] and Shiyu et al. [18]. The anticancer effect of fungal and bacterial strains was evaluated through cytotoxicity assay and pathological examination. The chemical composition of fungal and bacterial secondary metabolites was analyzed through GC mass spectrometry. The goal of this research is to evaluate the ability of some fungi and bacteria to produce secondary metabolites and testing their effect on specific cancer cell lines as a natural compounds.

2. Materials and methods

2.1 Cell lines

Human lung cancer (A549, ATCC, USA Catalogue number CCL-185), Human hepatocellular carcinoma (HepG2, ATCC, USA Catalogue number HB-8065) and Human breast adenocarcinoma (MCF7, ATCC, USA Catalogue number HTB-22) were kindly supplied from the International Center for Training and Advanced Research (ICTAR–Egypt).

The three human tumor cell lines were routinely maintained in Roswell Park Memorial Institute (RPMI) Medium supplied from Sigma-Aldrich-USA, supplemented with 10% Fetal Bovine Serum (FBS) supplied from Sigma-Aldrich-USA at 37°C in a humidified atmosphere containing 5% CO2 according to the producer protocol. Confluent sheets of different cell lines TC flasks were processed and maintained in 96 well plates and flasks according to the need.

2.2 Microorganisms

The fungal strains: *Aspergillus terreus (MT558939.1), Aspergillus fumigatus (MT635279.1), Aspergillus flavus (MT645322.1), Penicillium sp. Voucher AC11 (MT606192.1).* The bacterial strains: *Enterobacter cancerogenus (NR_044977.1), Bacillus subtilis spizizenii (NR_024931.1)* and *Bacillus paramycoides (NR_157734.1)* were supplied from faculty of Science-Ain Shams University-Microbiology Department. Organisms were cultured according to the culture protocol. Molecular identification of fungi and bacteria was done through Sigma Scientific Services Co. Cairo, Egypt, by DNA Sequencing.

2.3 Imatinib

It is a tyrosine kinase inhibitor used as a chemotherapeutic agent. Imatinib was supplied from Sigma-Aldrich-USA. It was solubilized in Dimethyl sulfoxide (DMSO) supplied from Sigma-Aldrich-USA. 100mg/ml. Cytotoxic effect was evaluated using MTT assay where test materials were 2 folds serially diluted on 24hrs pre-cultured cell lines treatment at 37°C post decanting growth medium. Treated cell lines were microscopically examined for detection of morphological changes and detached cells [19, 20, 21].

2.4 Molecular identification of the fungi and bacteria

2.4.1 DNA extraction from (fungi and bacteria)

DNA extraction was done according to the manufacturer instruction. “Sigma Scientific Services Co.” Cairo, Egypt. A volume of 200 µl of sample (liquid media that contains bacteria, fungi) was added in a microcentrifuge tube and 95 µl water were added, 95 µl solid tissue buffer (blue) and 10 µl proteinase K, sample was mixed thoroughly and then incubated at 55ºC for 2 hr. Sample was mixed thoroughly and was centrifuged at (12,000 ×g) for 1 min, tube was transferred to aqueous supernatant to a clean tube (300 µl). 600 µl Genomic Binding Buffer was added, mixed thoroughly. The mixture was transferred to a Zymo-Spin™ IIC-XL column in collection tube, centrifuged (≥ 12,000 ×g) for 1 min.

400 µl DNA pre- wash buffer was added to the column in a new collection tube and centrifuged at (12.000 ×g) for 1 min, a volume of 700 µl g-DNA wash buffer was added and centrifuged at (12.000 ×g) for 1 min, a volume of 200 µl g-DNA wash buffer was added and centrifuged at (12.000 ×g) for 1 min, a volume of 03 µl elution buffer incubate was added for 5 min, and then centrifuged at (12.000 ×g) for 1 min.

PCR reaction set-up, was done according to the manufacturer instruction. "Sigma Scientific Services Co." Fig. 22

PCR reaction set-up:

25 µL MyTaq Red Mix

8 µL DNA Template (change)

1 µl (20 Pico mol) Forward Primers

1 µl (20 Pico mol) Reverse Primers

15 µL Nuclease Free Water

Thermal Cycler Condition:

Step Temperature Time Cycles:

Initial denaturation	94 °C	6 min
Denaturation Annealing Extension	94 °C 56 °C 72 °C	45 s 45 s 35 cycle 1 min
Final Extension	72 °C	5 Mins

2.4.2 16S rRNA sequencing and data analysis

Sequencing to the PCR product on GATC Company (Jakob-Stadler-Platz 7 D-78467 Konstanz. Germany) was done via ABI 3730xl DNA sequencer (Jakob-Stadler-Platz 7 D-78467 Konstanz. Germany) by using forward and reverse primers according to the manufacturer's instruction. "Sigma Scientific Services Co." Fig. 22. Only by combining the traditional Sanger technology with the new 454 technology, can genomes now be sequenced and analyzed in half the usual project time, with a considerable reduction in the number of coatings and gaps. In addition, considerable cost advantages now make genome sequencing with the 454 technology accessible to the research community.

2.5 Secondary metabolite extraction

Selected endophyte cultures were inoculated into a 250 mL Erlenmeyer flask containing 100 mL of Potato Dextrose Broth (PDB) medium to grow the fungi. The flasks were kept in a 28 °C incubator for 2 weeks, during which time they were shaken periodically at 150 rpm. After the incubation period, 10% methanol was added to the fungi's fermentation broth to bring about homogenization.

Solvent extraction was used to remove the metabolite, and ethyl acetate and methanol were used as the organic solvents of choice. A solvent mixture of equal volume was added to the filtrate, stirred thoroughly for 10 minutes, & then left alone for 5 minutes, during which time 2 distinct, immiscible layers formed. Using a separating funnel, the compounds that were extracted from the solvent rose to the top. The crude metabolite was obtained by removing the solvent and drying the resulting compound in a rotator vacuum evaporator [22]. Dimethyl sulfoxide (DMSO) was used to dissolve the extract's crude solid residue, and the resulting solution was stored at 4 °C.

2.6 Detection of bioactive compounds by GC-MS analysis

TLC analysis helped clean up some of the impurities in the crude extract. Retention time, area%, molecular formula, & molecular weights of the various compounds were recognized & tabulated using GC-MS analysis of the partially purified crude Tables 1, 2, 3 and 5.

2.7 Determination of total protein

Total protein was determined using Bradford method [23]. Test sample and standard tubes were labeled. 0.15 milliliters of 0.85% Sodium Chloride Solution was added into the test tube marked "Blank." To the properly marked test tube, 0.2 ml of the prepared test sample solution was added. 2.2 ml of the Biuret Reagent was added in each test tube. After thoroughly combining, tubes were left to stand for 10 min at room temperature. One hundred microliter / ml of the Folin and Ciocalteau's Phenol Reagent was added to each tube. Tubes were thoroughly mixed/shaken directly after addition. For thirty min, the tubes were left at room temperature. After 30 min, the contents of the test tubes were moved to a microplate and were read the absorbance. Absorbance at 595 nm can be measured with a spectrophotometer or a smartphone camera (using the RGBradford method) after only 5 minutes of incubation. From the Standard curve, the protein concentration (mg/ml) can be calculated in each sample.

2.8 Cytotoxicity assay

Assaying cell viability using [3 - (4, 5-dimethylthiazol-2-yl) 2, 5 diphenyl tetrazolium bromide (MTT) supplied from Sigma-Aldrich-USA. A solubilization solution dimethyl sulfoxide (DMSO) supplied from Sigma-Aldrich-USA. And a spectrophotometer supplied from Biotech engineering-UK.

Treated cell lines were analyzed microscopically. Phosphate buffered saline supplied from Biowhittaker-Belgium. The ELISA plate reader (ELX-8000, Biotek, USA) was used to measure the optical densities. Using the Master-plex-2010 software, the IC_{50} values of the test extracts were calculated. Results from three separate tests were presented [24].

The percentage of survival was calculated according to the following equation:

$$\% \text{ viability} = \frac{X^{-} \text{ OD of treated cells}}{X^{-} \text{ OD of untreated cells}} \times 100$$

X^{-} : mean average

OD: optical density

2.9 Microscopic examination

Cancer cells pre-cultured tissue culture flasks (TCF) and metabolites IC_{50} values treated, and untreated cells were used as negative control. 24-hour post-treatment morphological alterations were detected with a light microscope [Hund, Germany]. Hematoxylin and eosin staining were used for the analysis of pathological changes after therapy [25].

2.10 Gas chromatography mass spectrum (GCMS)

Secondary metabolites were analyzed for their chemical make-up using a Trace GC1310-ISQ mass spectrometer (Thermo Scientific, Austin, TX, USA) coupled to a direct capillary column TG-5MS (30 metres in length, 0.25 millimetres in diameter, and 0.030 micrometres in film thickness). Starting with a temperature of 50 degrees Celsius, the column oven was heated at a rate of 5 degrees Celsius per minute until it reached 230 degrees Celsius, where it was maintained for two minutes. From there, it was heated at a rate of 30 degrees Celsius per minute until it reached 290 degrees Celsius.

There was a steady flow of 1 ml/min of Helium utilized as the carrier gas, and the injector and MS transfer line temperatures were maintained at 250°C and 260°C, respectively. An Auto sampler AS1300 combined with a GC operating in split mode was used to inject diluted samples of 1 µl at a 3 minute solvent delay. Mass spectra were acquired using an EI detector at ionization voltages of 70 eV, scanning from m/z 40 to 1000. It was decided to use an ion source with a temperature of 200 °C.

The retention times & mass spectra of the components were compared to those in the WILEY 9 and NIST 11 mass spectral databases, allowing for their identification [7].

2.11 Statistical analysis

The statistical software for the social sciences, version 20.0, was used to analyze the collected data (SPSS Inc., Chicago, Illinois, USA). Averages and standard deviations were used to summarize numerical information (SD). Quantitative information was presented as a proportion of the whole, and qualitative information as a frequency distribution.

3. Results

3.1 Gas chromatography mass spectrum analysis (GCMS)

GCMS analysis showed the different derivative compound released post fungal and bacterial extraction, the different compounds were listed in (Tables 1, 2, 3 and 5).

3.2 Cytotoxicity

The cytotoxic effect of derived fungal metabolites showed variable inhibitory concentrations of cellular proliferation that was metabolite and cell type dependent, and so long as the viability was went up, the concentration was lowered Fig. 1. Data recorded revealed that MCF7 significantly ($P<0.05$) influenced by *Asp. terreus* metabolite than HepG2 and A549 recording IC_{50} value of 114 µg/ ml, 235 µg/ ml and 485 µg/ml respectively. Similarly, MCF7 was significantly influenced by *Asp. flavus* ($P<0.05$) than A549 and HepG2 respectively. In the meantime, A549 cells was significantly influenced by *Asp. Fumigatus* ($P<0.05$) than HepG2 and MCF7 (Table 4 and Figures. 1, 2).

3.3 Microscopic examination (pathology)

3.3.1 fungi

Assessment of pathological changes using hematoxylin and eosin staining, (H and E, Original magnification 100X, Oil), showed that: The untreated control A549, HepG2 and MCF7 cells showed regular cells with hyperchromatic nuclei & nuclear and cellular pleomorphism Fig. 3. Imatinib treated A549 cell line showed necrotic cells with mixed euochromatin & heterochromatin, Irregularities of cellular and nuclear outlines and apoptotic bodies. Fig. 4.

A549 treated Necrotic cells with euchromatin & heterochromatin (red arrows), broken membranes (green arrows), intranuclear eosinophyllic structures (orange arrows), and shrunken apoptotic cells with uneven cell and nuclear membranes were all features of Aspergillus terreus (Black arrows). Fig. 3. Also, the same cell line treated *Aspergillus flavus* treated cell line showed shrunken apoptotic cells with shrunken nuclei (Yellow arrows), and irregular cell membranes (Red arrows), peripheral condensation of chromatin (Green arrow). Fig. 3. similarly**,** the same cell line treated with *Aspergillus fumigatus* showed shrunken apoptic cells with shrunken nuclei (Yellow arrows), and irregular cell membranes (Red arrows), peripheral condensation of chromatin (Green arrows). Fig. 3. Similarly, HepG2 cell line treated with a chemotherapeutic agent Imatinib found out swollen necrotic cells with mixed euochromatin & heterochromatin and irregular outline.

Cell debris and apoptotic bodies also seen. A photomicrograph showing swollen necrotic cells with mixed euochromatin and heterochromatin. Fig. 4. Meanwhile, *Aspergillus terreus* treatment of the HepG2 cell line resulted in bloated cells, enlarged nuclei containing both euchromatin and heterochromatin, & broken cell membranes (Yellow arrows) (Green arrows). Eosinophyll granules are eosinophyll-like structures found inside of cells (Red arrows). Fig. 3. There were also necrotic swelling cells with mixed euochromatin and heterochromatin & a burst cell membrane in the same cell line that had been treated with *Aspergillus flavus* (Blue arrows) (Red arrow). Fig. 3. Necrotic enlarged cells, enlarged nuclei with mixed euchromatin and heterochromatin, and burst cell membranes were also detected in the same cell line exposed to *Aspergillus fumigatus* (Blue arrows).

Condensed chromatin at the cell's periphery and shrunken, apoptotic nuclei shown by green arrows (Orange arrow). Cell membrane rupture and chromatin condensation at the periphery characterize secondary necrosis (Yellow arrows). Remains of apoptosis (Red arrows). Fig. 3. Concurrently, MCF7 cells exposed to Imatinib exhibited nuclear fragmentation, inflated necrotic cells with mixed euochromatin, heterochromatin, & shrinking apoptotic cells, as well as abnormalities of cellular and nuclear outlines and membrane blebbing.

Also present: apoptotic bodies. Photomicrograph demonstrating irregularities in cellular and nuclear outlines (Blue arrow), membrane blebbing (orange arrow), and apoptotic bodies (green arrows) as well as shrunken apoptotic cells (Green arrows) (Black arrow). Fig. 4. Also, MCF7 treated *Aspergillus terreus* showed necrotic cells with ruptured cell membranes (Red arrows), and mixed euchromatin and heterochromatin (Green arrows). Intracellular eosinophyllic structures (Black arrows). Fig. 3. Also, the same cell line treated *Aspergillus flavus* showed shrunken apoptotic cells and shrunken nuclei (Red arrows), peripheral condensation of chromatin (Green arrows) and nuclear fragmentation (Yellow arrow). Fig. 3. similarly**,** the same cell line treated with *Aspergillus fumigatus* showed shrunken apoptotic cells with shrunken nuclei (Red arrows) and apoptotic bodies (Green arrows). Fig. 3. [1].

3.3.2 Bacteria

A549 cell lines were showed significantly a reduced IC_{50} values ($P<0.05$) to *Bacillus paramycoides,* compared with that of *Bacillus subtilis spizizenii* and *Enterobacter cancerogenus* respectively**.** Similarly, HepG2 cell line showed a significantly reduced IC_{50} value ($P<0.05$) to *Bacillus paramycoides,* compared with that of *Enterobacter cancerogenus* and *Bacillus subtilis spizizenii***.** In the meantime, MCF7 cell line showed a significantly reduced IC_{50} value ($P<0.05$) of *Bacillus paramycoides* metabolite compared to that of *Enterobacter cancerogenus* ($P<0.05$) reduced IC_{50} values against *Bacillus paramycoides* and *Enterobacter cancerogenus* metabolites compared with both A549 and MCF7 (Table 6 and Fig 5, 6).

Evaluation of pathological changes using hematoxylin and eosin staining showed that no treatment condition normal cells with hyperchromatic nuclei and nuclear and cellular pleomorphism were seen in MCF7, HepG2, and A549 cells. Fig. 7. A549 cell line treated with a chemotherapeutic agent Imatinib showed necrotic cells with mixed euochromatin and heterochromatin, Irregularities of cellular and nuclear outlines and apoptotic bodies Fig. 4. On the other hand, A549 cell line treated with *Bacillus paramycoides* showed shrunken apoptotic cells with irregular cell membrane and peripheral condensation of chromatin Fig. 7.

Also, HepG2 cell line treated with Imatinib indicated swollen necrotic cells with mixed euochromatin and heterochromatin and irregular outline. Cell debris and apoptotic bodies were also seen. A photomicrograph showed swollen necrotic cells with mixed euochromatin and heterochromatin Fig. 4. On the other hand, HepG2 cell line treated with *Bacillus paramycoides* showed shrunken apoptotic cells with peripheral condensation of chromatin. Fig. 7. MCF7cell line treated with Imatinib showed nuclear fragmentation, swollen necrotic cells with mixed euochromatin, heterochromatin and shrunken apoptotic cells, irregularities of cellular and nuclear outlines and membrane blebbing.

Apoptotic bodies also were seen. A photomicrograph showed shrunken apoptotic cells, nuclear fragmentation, swollen necrotic cells with mixed euochromatin and heterochromatin, irregularities of cellular and nuclear outlines, membrane blebbing and apoptotic bodies. Fig. 4. On the other hand, MCF7 treated *Bacillus paramycoides* showed shrunken apoptotic epithelial cells with peripheral condensation of chromatin Fig. 7. [1].

3.4 Molecular identification of the selected organisms

4. Discussion

The incidence of cancer continues to rise, and it is now recognized as one of the top causes of mortality worldwide, despite breakthroughs in cancer therapy and detection. The normal cells of the body might be damaged by the chemotherapeutic drugs used to treat cancer. There is also the issue of medication resistance developing in cells that have been exposed to chemotherapy. Because of the side effects of chemotherapy, researchers are interested in learning more about how to harness the microbiome and its secondary metabolites for cancer treatment [1].

Many secondary metabolites with pharmacological, therapeutic, pesticidal, and phytocidal potential are produced by microorganisms [7, 11, 17]. Fungi and bacteria characterized by synthesize of secondary metabolites which are low molecular mass products, not essential for growth of the organism, but very important for human health. They include antibiotics, antitumor agents, cholesterol lowering drugs, and others [3, 14]. There are many reasons for studying the secondary metabolites of microorganisms for biological activity.

First, bacteria and fungi have existed for over a billion years. During this time, they have evolved biosynthetic pathways and mechanisms for synthesizing a rich arsenal of complex secondary metabolites. Most of these compounds interact with enzyme targets and help the organism survive against a wide array of challenges. Each new microbe has the potential for yielding as-yet undiscovered compounds with bioactivity that can be adapted for medicinal purposes. It has been estimated that fewer than 16% of the fungal species that have been described have been cultured and studied. These described species probably represent fewer than 5% of the total fungal species that await exploration [7, 13].

Chemotherapeutic agents used for cancer treatment possess non- specific toxicity to the normal body cells. Also, body cells exposed to chemotherapy become resistant to drugs. In order to find compounds that can stop, slow, or reverse the carcinogenic process while still being safe for human use, interdisciplinary groups must work together for cancer chemoprevention. As lemongrass is a fragrant grass, its essential oil is employed in the pharmaceutical industry and to treat a variability of maladies using more holistic, non-conventional approaches [26].

Chakrabhavi et al. [9] and Saadia et al. [12] reported that *Aspergillus terreus, Aspergillus awamoic EM66* and *Penicillium janthinellum* had anticancer activity. These results are similar to the present results of the study. On the other hand, *Bacillus paramycoides* was the most effective bacteria in treatment of A549, HepG2 and MCF7 as reported by Matthew et al. [27]. It is not clear how *Aspergillus* and imatinib, or *Bacillus paramycoids* and imatinib, would interact when applied to MCF7, HepG2, and A549 cells under a microscope. These cells are commonly used in research, but there is no information available on the effects of *Aspergillus, Bacillus paramycoids*, or imatinib on these cell lines [20].

Aspergillus is a type of fungus that can cause infections in people with compromised immune systems. It can cause a variety of symptoms, including fever, cough, and difficulty breathing, and can be serious if not treated promptly [28, 29]. Imatinib is a chemotherapy drug that is used to treat certain types of cancer, including certain kinds of leukemia and gastrointestinal stromal tumors [21].

Inhibiting enzymes that promote cancer cell growth and division is how it works [19]. *Bacillus paramycoids* is a type of bacteria that is found in soil and water. It is not known to cause disease in humans, but it has been found to be pathogenic in some animals [30]. Exciting new findings suggest microorganisms may be useful therapeutic agents in the fight against cancer. The growth of tumors can be slowed by certain chemicals generated by bacteria called derived metabolites [4, 10, 18, 31]. These findings corroborate those we obtained.

This research shows revealed that MCF7 significantly (P<0.05) influenced by *Asp. terreus* metabolite than HepG2 and A549 recording IC_{50} value of 114 µg/ ml, 235 µg/ ml and 485 µg/ml respectively. Similarly, MCF7 was significantly influenced by *Asp. flavus* (P<0.05) than A549 and HepG2 respectively. In the meantime, A549 cells was significantly influenced by *Aspergillus fumigatus* (P<0.05) than HepG2 and MCF7. Similarly, Ahmed et al. [32] reported that the strong growth inhibition of human hepatoma cells of *Aspergillus fumigatus* metabolites resulted by promoting cell apoptosis resulting in the dramatic change from polygonal cells to rounded ones. Ahmed et al. [33] found that, the pure bioactive compounds from *Aspergillus terreus* and *Curvularia lunata* induced different morphologically changes on HepG2, A549 and HEp-2 by promoting cell apoptosis.

Imatinib treated A549 cell line showed necrotic cells with mixed euochromatin & heterochromatin, Irregularities of cellular and nuclear outlines and apoptotic bodies. Abdel Aziz et al. [34] reported the treatment of HCT116 cells with 10 µM imatinib (p < 0.05) for 72 hours was related to nuclear fragmentation and significant increase in caspase 3 activity by 1.14- and 1.52-fold compared to the control cells. The first study indicating imatinib triggered the autophagy mechanism of mammalian cells did so by Ertmer et al. [35] and showed a dose-dependent effect. Imatinib's cytotoxicity in GIST was diminished because it activated autophagy as a survival strategy in quiescent cells. Treatment of glioblastoma cells with low or high concentrations of imatinib led to cell growth arrest & apoptosis, respectively, as reported in a recent study by Kim et al. [36].

The present study confirmed previous research showing that imatinib inhibits cell metastasis at concentrations as low as 1-10 M and induces apoptosis at higher doses (20-100 M). These findings corroborate the efficacy and utility of imatinib as a chemotherapeutic drug in human CRC cell lines HT29, HepG2, and MCF7, as reported by Attoub et al. [37]. We have covered the total ethanolic derived metabolites those showed anticancer activity discovered from endophytic Fungal and Bacterial metabolites. The compounds have been listed based on their name, area %, formula, and their molecular weight. The present data were in agreement with Ashish et al. [7].

A549 cell lines were significantly (P<0.05) showed a reduced IC_{50} values to *Bacillus paramycoides*, compared with that of *Bacillus subtilis spizizenii* and *Enterobacter cancerogenus* respectively. Similarly, HepG2 cell line showed a significantly (P<0.05) reduced IC_{50} value to *Bacillus paramycoides,* compared with that of *Enterobacter cancerogenus* and *Bacillus subtilis spizizenii*. In the meantime, MCF7 cell line showed a significantly reduced (P<0.05) IC_{50} value of *Bacillus paramycoides* metabolite compared to that of *Enterobacter cancerogenus* (P<0.05) reduced IC_{50} values against *Bacillus paramycoides* and *Enterobacter cancerogenus* metabolites compared with both A549 and MCF7

Cell cycle arrest, apoptosis, growth suppression, and metastasis arrest are just some of the ways in which *Bacillus paramycoides* has recently been proven to reduce cancer progression [38]. The anti-fungal actions of *Bacillus lipopeptides*, such as subtilisin, paramycoidesin, and iturin A, have been linked to the activation of apoptosis via a mitochondria-dependent pathway, as reported by Dey et al. [39] he found that lipopeptides from *Bacillus subtilis*, primarily iturin, suppress the growth of A549 lung cancer cells. *Bacillus lipopeptides* has been shown to have a scale of variability of therapeutic effects, including anti-inflammation, anti-cancer, neuroprotective properties, suppression of platelet aggregation, and immunomodulation therapy for diabetes, according to a number of studies [40]. *Bacillus lipopeptides* have been shown to exhibit anti-cancer impact on both MCF-7 human breast cancer cells and H460 human lung cancer cells [41, 42].

An extremely rapid metabolic rate is one of Bacillus' most recognizable characteristics, which positions it amongst the most well-known producers of natural products. *Bacillus* species produce a number of essential metabolites, including as the cyclic lipopeptide antibiotics iturin, surfactin, and fengycin. Some of these natural compounds, like surfactin, streptavidin, and bacillimycin D, have the potential to be used in cancer treatment. However, additional research is necessary to determine the unknown possible biological activities of certain other components [43].

5. Conclusion

In the present work, the anticancer effect of several fungal and bacterial secondary metabolites was examined on cancer cell lines (A549, HepG2, and MCF-7). In A549, HepG2, and MCF-7 cells, bacterial and fungal metabolites drastically lowered the percentage of viable cells. Results indicated that bacterial and fungal metabolites exhibited the strongest anticancer effect against human cancer cells A549, HepG2, and MCF-7.

It has been demonstrated that secondary metabolites have anticancer properties. The toxicity of derived products is based on the product and cancer cell line. Pathological modifications of bacterial and fungal metabolites were metabolite- and cell-type-dependent.

6. Recommendation

It can be recommended that both drugs and derived metabolites can be used in cancer therapy. Nano formulation of derived metabolites is recommended to evaluate the enhancement of anticancer potential. Combination of derived metabolites with chemotherapy and evaluate the sole application from the combined form. Preclinical In vivo application of derived metabolites is recommended. Monitoring of the anticancer potential of derived bacterial and fungal metabolites in combined forms.

7. Conflicts of interest

The authors declare there are no conflicts of interest.

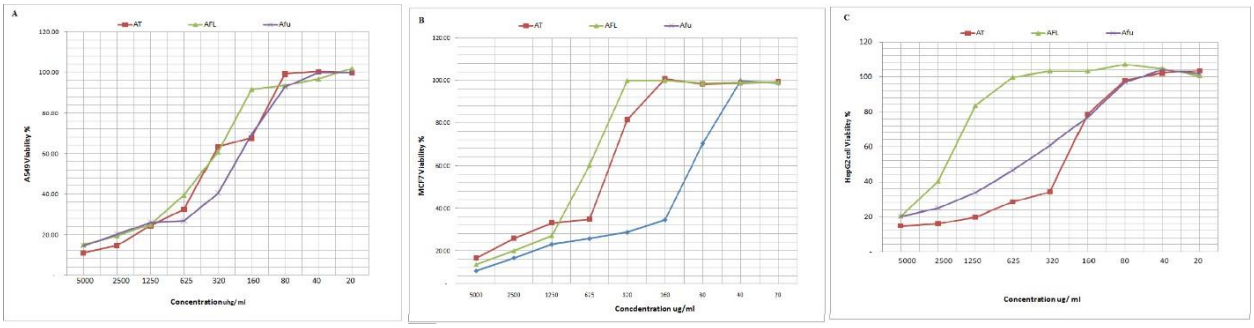

Fig. 1 Comparison between *Aspergillus terreus, Aspergillus flavus and Aspergillus fumigatus* toxicity on treated A549, HepG2 and MCF7 relative to concentration.

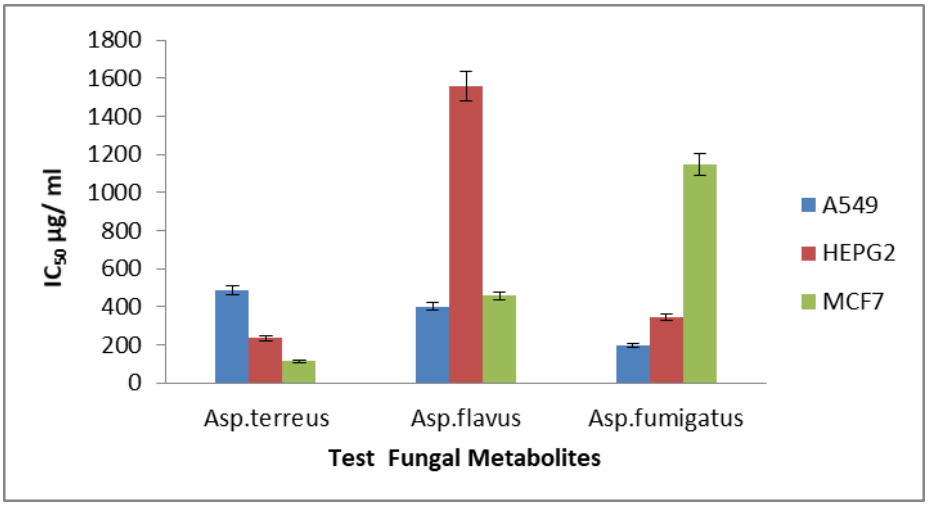

Fig. 2 Comparison between *Aspergillus terreus, Aspergillus flavus and Aspergillus fumigatus* secondary metabolites IC_{50} values in treated A549, HepG2 and MCF7.

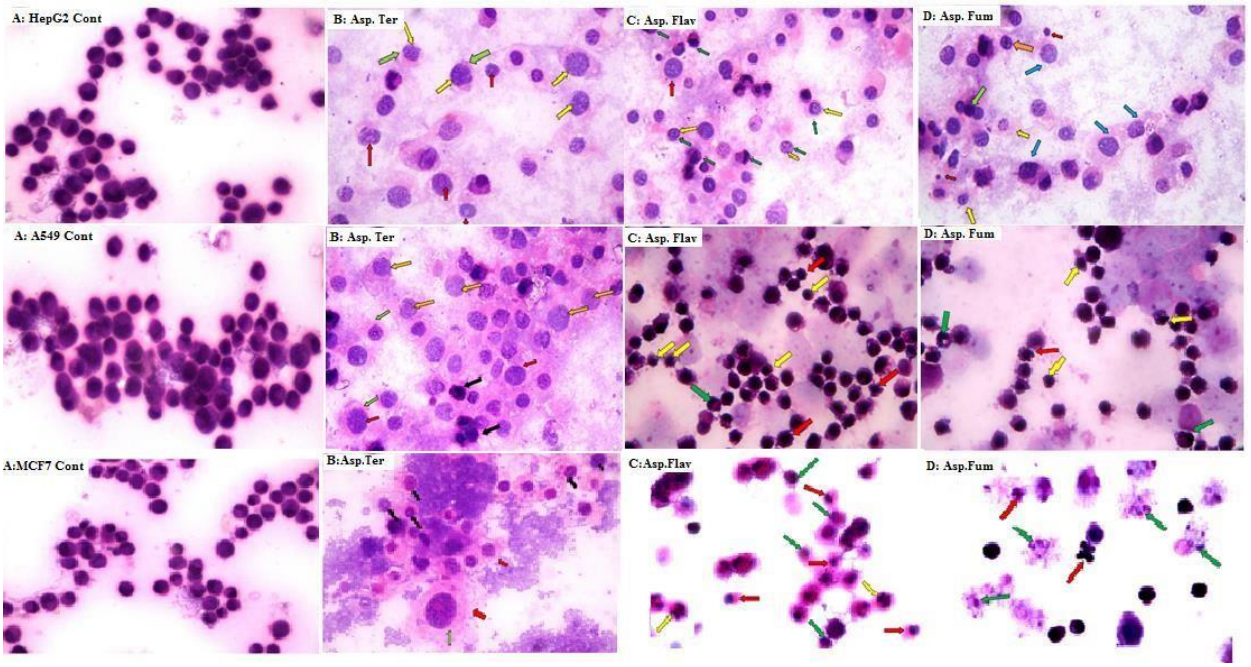

Fig. 3 Comparison between untreated control A549, HepG2 and MCF7cell lines and treated cell lines with *Aspergillus terreus, Aspergillus flavus* and *Aspergillus fumigatus.*

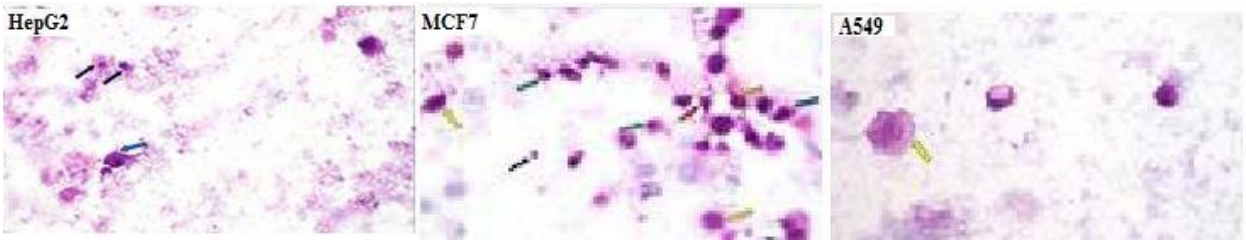

Fig. 4 Imatinib treated cell lines showed shrunken apoptotic cells (Green arrows), nuclear fragmentation (Red arrow), swollen necrotic cells with mixed euochromatin and heterochromatin (Yellow arrows), irregularities of cellular and nuclear outlines (Blue arrow), membrane blebbing (orange arrow) and apoptotic bodies (Black arrow).

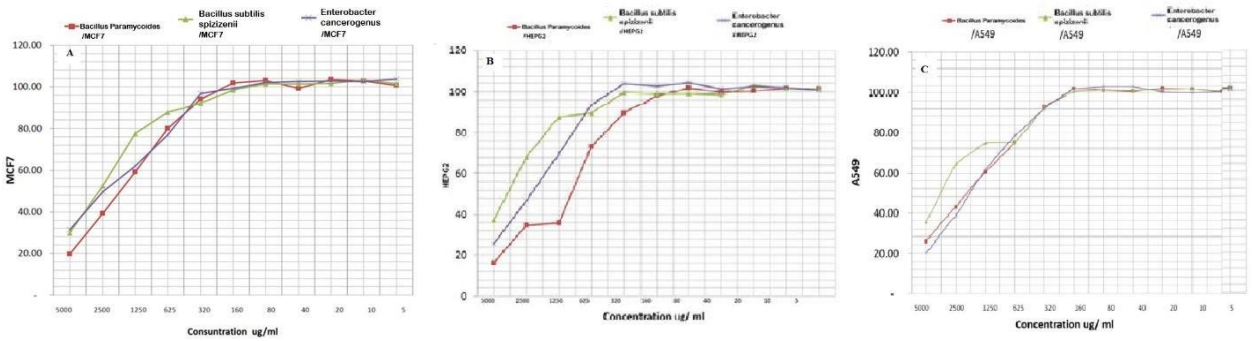

Fig. 5 Comparison between *Bacillus paramycoides, Bacillus subtilis spizizenii,* and *Enterobacter cancerogenus* toxicity on treated A549, HepG2 and MCF7 relative to concentration.

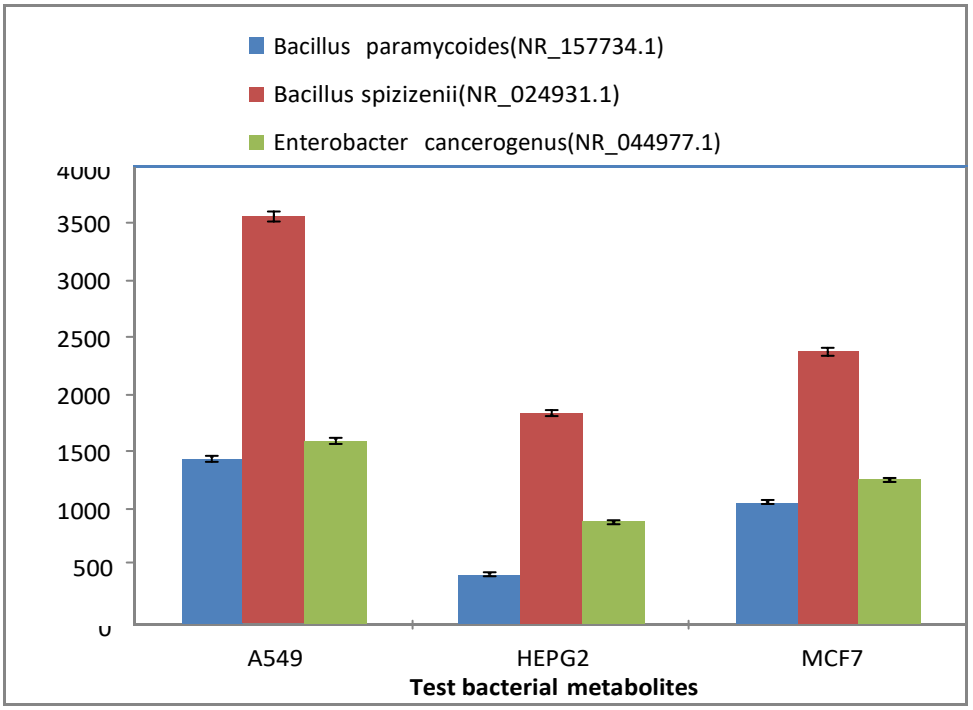

Fig. 6 Comparison between *Bacillus paramycoides, Bacillus subtilis spizizenii,* and *Enterobacter cancerogenus* secondary metabolites IC_{50} values in treated A549, HepG2, and MCF7.

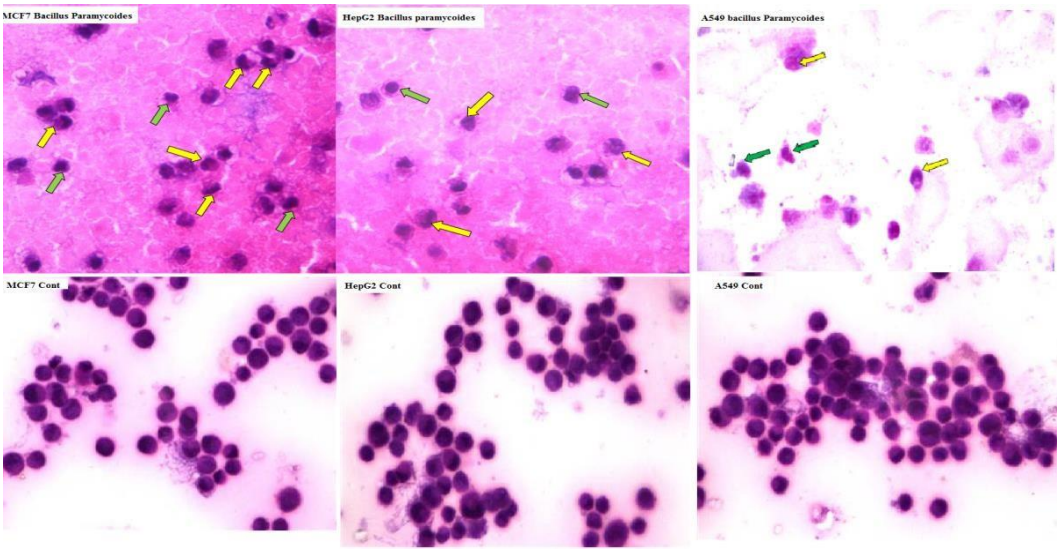

Fig. 7 Comparison between untreated control A549, HepG2 and MCF7 cell lines and treated cell lines with *Bacillus paramycoides.*

Description	Max Score	Total Score	Query Cover	E value	Per. Ident	Accession
Penicillium sp. voucher AC11 internal transcribed spacer 1, partial sequence; 5.8S ribosomal RNA gene and internal transcribed spacer 2, complete sequ	846	846	100%	0.0	100.00%	MT606192.1
Penicillium expansum strain DUCC5734 small subunit ribosomal RNA gene, partial sequence; internal transcribed spacer 1, 5.8S ribosomal RNA gene, a	846	846	100%	0.0	100.00%	MT582774.1
Penicillium crustosum strain DUCC5730 internal transcribed spacer 1, partial sequence; 5.8S ribosomal RNA gene and internal transcribed spacer 2, con	846	846	100%	0.0	100.00%	MT582770.1
Penicillium crustosum strain DTO 403-D6 small subunit ribosomal RNA gene, partial sequence; internal transcribed spacer 1, 5.8S ribosomal RNA gene,	846	846	100%	0.0	100.00%	MT316358.1
Penicillium crustosum strain YT-9 internal transcribed spacer 1, partial sequence; 5.8S ribosomal RNA gene and internal transcribed spacer 2, complete s	846	846	100%	0.0	100.00%	MT477711.1
Penicillium sp. strain ZMQL5 small subunit ribosomal RNA gene, partial sequence; internal transcribed spacer 1, 5.8S ribosomal RNA gene, and internal t	846	846	100%	0.0	100.00%	MT446164.1
Penicillium commune isolate 4RM0 internal transcribed spacer 1, partial sequence; 5.8S ribosomal RNA gene and internal transcribed spacer 2, complete	846	846	100%	0.0	100.00%	MT300172.1
Penicillium crustosum voucher Pen c10 internal transcribed spacer 1, partial sequence; 5.8S ribosomal RNA gene and internal transcribed spacer 2, com	846	846	100%	0.0	100.00%	MT298917.1
Penicillium crustosum voucher Pen c09 internal transcribed spacer 1, partial sequence; 5.8S ribosomal RNA gene and internal transcribed spacer 2, com	846	846	100%	0.0	100.00%	MT298916.1
Penicillium crustosum voucher Pen c08 internal transcribed spacer 1, partial sequence; 5.8S ribosomal RNA gene and internal transcribed spacer 2, com	846	846	100%	0.0	100.00%	MT298915.1
Penicillium crustosum voucher Pen c07 internal transcribed spacer 1, partial sequence; 5.8S ribosomal RNA gene and internal transcribed spacer 2, com	846	846	100%	0.0	100.00%	MT298914.1
Penicillium crustosum voucher Pen c06 internal transcribed spacer 1, partial sequence; 5.8S ribosomal RNA gene and internal transcribed spacer 2, com	846	846	100%	0.0	100.00%	MT298913.1
Penicillium crustosum voucher Pen c05 internal transcribed spacer 1, partial sequence; 5.8S ribosomal RNA gene and internal transcribed spacer 2, com	846	846	100%	0.0	100.00%	MT298912.1
Penicillium crustosum voucher Pen c04 internal transcribed spacer 1, partial sequence; 5.8S ribosomal RNA gene and internal transcribed spacer 2, com	846	846	100%	0.0	100.00%	MT298911.1
Penicillium crustosum voucher Pen c03 internal transcribed spacer 1, partial sequence; 5.8S ribosomal RNA gene and internal transcribed spacer 2, com	846	846	100%	0.0	100.00%	MT298910.1
Penicillium crustosum voucher Pen c02 internal transcribed spacer 1, partial sequence; 5.8S ribosomal RNA gene and internal transcribed spacer 2, com	846	846	100%	0.0	100.00%	MT298909.1
Penicillium expansum voucher Pen 18 small subunit ribosomal RNA gene, partial sequence; internal transcribed spacer 1, 5.8S ribosomal RNA gene, and	846	846	100%	0.0	100.00%	MT294667.1
Penicillium expansum voucher Pen 17 small subunit ribosomal RNA gene, partial sequence; internal transcribed spacer 1, 5.8S ribosomal RNA gene, and	846	846	100%	0.0	100.00%	MT294666.1
Penicillium expansum voucher Pen 11 small subunit ribosomal RNA gene, partial sequence; internal transcribed spacer 1, 5.8S ribosomal RNA gene, and	846	846	100%	0.0	100.00%	MT294665.1

Fig. 8 *Penicillium sp. voucher AC11(MT606192.1)* internal transcribed spacer 1, partial sequence; 5.8S ribosomal RNA gene and internal transcribed spacer 2, complete sequence; and large subunit ribosomal RNA gene, partial sequence.

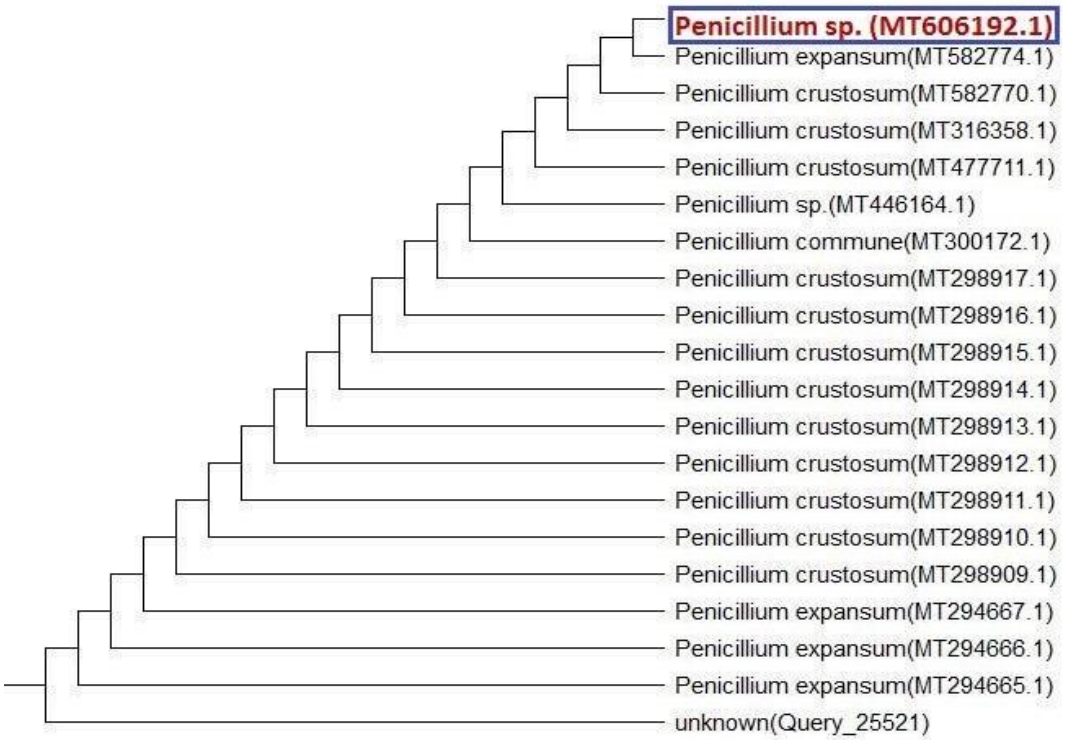

Fig. 9 Phylogenetic tree of *Penicillium sp. Voucher AC11 (MT606192.1).*

Description	Max Score	Total Score	Query Cover	E value	Per. Ident	Accession
Aspergillus fumigatus small subunit ribosomal RNA gene, partial sequence; internal transcribed spacer 1, 5.8S ribosomal RNA gene, and internal transcri	863	863	100%	0.0	100.00%	MT635279.1
Trametes elegans isolate MEBP0066 small subunit ribosomal RNA gene, partial sequence; internal transcribed spacer 1, 5.8S ribosomal RNA gene, and	863	863	100%	0.0	100.00%	MT597442.1
Aspergillus fumigatus isolate MEBP0082 small subunit ribosomal RNA gene, partial sequence; internal transcribed spacer 1 and 5.8S ribosomal RNA ger	863	863	100%	0.0	100.00%	MT597433.1
Aspergillus fumigatus isolate MEBP0074 small subunit ribosomal RNA gene, partial sequence; internal transcribed spacer 1, 5.8S ribosomal RNA gene, a	863	863	100%	0.0	100.00%	MT597427.1
Aspergillus fumigatus isolate MEBP0062 internal transcribed spacer 1, partial sequence; 5.8S ribosomal RNA gene and internal transcribed spacer 2, cor	863	863	100%	0.0	100.00%	MT593013.1
Aspergillus fumigatus isolate MEBP0063 small subunit ribosomal RNA gene, partial sequence; internal transcribed spacer 1, 5.8S ribosomal RNA gene, a	863	863	100%	0.0	100.00%	MT591987.1
Aspergillus oerlinghausenensis isolate 2011F22 small subunit ribosomal RNA gene, partial sequence; internal transcribed spacer 1, 5.8S ribosomal RNA	863	863	100%	0.0	100.00%	MT558945.1
Aspergillus fumigatus isolate 2011F6 small subunit ribosomal RNA gene, partial sequence; internal transcribed spacer 1, 5.8S ribosomal RNA gene, and i	863	863	100%	0.0	100.00%	MT558940.1
Aspergillus fumigatus clone SF_991 small subunit ribosomal RNA gene, partial sequence; internal transcribed spacer 1, 5.8S ribosomal RNA gene, and ir	863	863	100%	0.0	100.00%	MT530267.1
Aspergillus fumigatus clone SF_588 small subunit ribosomal RNA gene, partial sequence; internal transcribed spacer 1, 5.8S ribosomal RNA gene, and ir	863	863	100%	0.0	100.00%	MT529864.1
Aspergillus fumigatus clone SF_501 small subunit ribosomal RNA gene, partial sequence; internal transcribed spacer 1, 5.8S ribosomal RNA gene, and ir	863	863	100%	0.0	100.00%	MT529777.1
Aspergillus fumigatus clone SF_209 small subunit ribosomal RNA gene, partial sequence; internal transcribed spacer 1, 5.8S ribosomal RNA gene, and ir	863	863	100%	0.0	100.00%	MT529485.1
Aspergillus fumigatus clone SF_202 small subunit ribosomal RNA gene, partial sequence; internal transcribed spacer 1, 5.8S ribosomal RNA gene, and ir	863	863	100%	0.0	100.00%	MT529478.1
Aspergillus fumigatus clone SF_190 small subunit ribosomal RNA gene, partial sequence; internal transcribed spacer 1, 5.8S ribosomal RNA gene, and ir	863	863	100%	0.0	100.00%	MT529466.1
Aspergillus fumigatus clone SF_189 internal transcribed spacer 1, partial sequence; 5.8S ribosomal RNA gene and internal transcribed spacer 2, complet	863	863	100%	0.0	100.00%	MT529465.1
Aspergillus fumigatus clone SF_173 internal transcribed spacer 1, partial sequence; 5.8S ribosomal RNA gene and internal transcribed spacer 2, complet	863	863	100%	0.0	100.00%	MT529449.1
Aspergillus fumigatus clone SF_172 small subunit ribosomal RNA gene, partial sequence; internal transcribed spacer 1, 5.8S ribosomal RNA gene, and ir	863	863	100%	0.0	100.00%	MT529448.1
Aspergillus fumigatus clone SF_171 internal transcribed spacer 1, partial sequence; 5.8S ribosomal RNA gene and internal transcribed spacer 2, complet	863	863	100%	0.0	100.00%	MT529447.1
Aspergillus fumigatus clone SF_169 internal transcribed spacer 1, partial sequence; 5.8S ribosomal RNA gene and internal transcribed spacer 2, complet	863	863	100%	0.0	100.00%	MT529445.1

Fig. 10 *Aspergillus fumigatus (MT635279.1)* small subunit ribosomal RNA gene, partial sequence; internal transcribed spacer 1, 5.8S ribosomal RNA gene, and internal transcribed spacer 2, complete sequence; and large subunit ribosomal RNA gene, partial sequence.

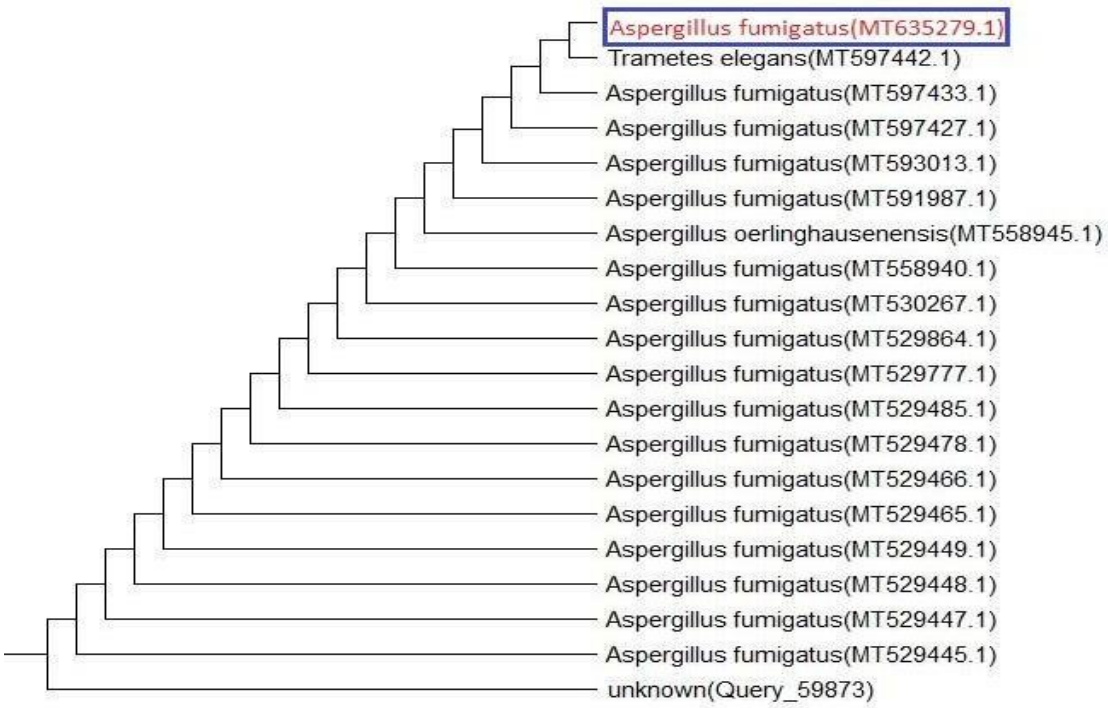

Fig. 11 Phylogenetic tree of *Aspergillus fumigatus (MT635279.1).*

Description	Max Score	Total Score	Query Cover	E value	Per. Ident	Accession
Aspergillus terreus isolate 2011F5 small subunit ribosomal RNA gene, partial sequence; internal transcribed spacer 1, 5.8S ribosomal RNA gene, and inte	963	963	100%	0.0	100.00%	MT558939.1
Aspergillus terreus clone SF_981 small subunit ribosomal RNA gene, partial sequence; internal transcribed spacer 1, 5.8S ribosomal RNA gene, and inte	963	963	100%	0.0	100.00%	MT530257.1
Aspergillus terreus clone SF_977 small subunit ribosomal RNA gene, partial sequence; internal transcribed spacer 1, 5.8S ribosomal RNA gene, and inte	963	963	100%	0.0	100.00%	MT530253.1
Aspergillus terreus clone SF_963 small subunit ribosomal RNA gene, partial sequence; internal transcribed spacer 1, 5.8S ribosomal RNA gene, and inte	963	963	100%	0.0	100.00%	MT530239.1
Aspergillus terreus clone SF_960 small subunit ribosomal RNA gene, partial sequence; internal transcribed spacer 1, 5.8S ribosomal RNA gene, and inte	963	963	100%	0.0	100.00%	MT530236.1
Aspergillus terreus clone SF_954 small subunit ribosomal RNA gene, partial sequence; internal transcribed spacer 1, 5.8S ribosomal RNA gene, and inte	963	963	100%	0.0	100.00%	MT530230.1
Aspergillus terreus clone SF_940 small subunit ribosomal RNA gene, partial sequence; internal transcribed spacer 1, 5.8S ribosomal RNA gene, and inte	963	963	100%	0.0	100.00%	MT530216.1
Aspergillus terreus clone SF_938 small subunit ribosomal RNA gene, partial sequence; internal transcribed spacer 1, 5.8S ribosomal RNA gene, and inte	963	963	100%	0.0	100.00%	MT530214.1
Aspergillus terreus clone SF_932 small subunit ribosomal RNA gene, partial sequence; internal transcribed spacer 1, 5.8S ribosomal RNA gene, and inte	963	963	100%	0.0	100.00%	MT530208.1
Aspergillus terreus clone SF_928 small subunit ribosomal RNA gene, partial sequence; internal transcribed spacer 1, 5.8S ribosomal RNA gene, and inte	963	963	100%	0.0	100.00%	MT530204.1
Aspergillus terreus clone SF_925 small subunit ribosomal RNA gene, partial sequence; internal transcribed spacer 1, 5.8S ribosomal RNA gene, and inte	963	963	100%	0.0	100.00%	MT530201.1
Aspergillus terreus clone SF_923 small subunit ribosomal RNA gene, partial sequence; internal transcribed spacer 1, 5.8S ribosomal RNA gene, and inte	963	963	100%	0.0	100.00%	MT530199.1
Aspergillus terreus clone SF_921 small subunit ribosomal RNA gene, partial sequence; internal transcribed spacer 1, 5.8S ribosomal RNA gene, and inte	963	963	100%	0.0	100.00%	MT530197.1
Aspergillus terreus clone SF_920 small subunit ribosomal RNA gene, partial sequence; internal transcribed spacer 1, 5.8S ribosomal RNA gene, and inte	963	963	100%	0.0	100.00%	MT530196.1
Aspergillus terreus clone SF_918 small subunit ribosomal RNA gene, partial sequence; internal transcribed spacer 1, 5.8S ribosomal RNA gene, and inte	963	963	100%	0.0	100.00%	MT530194.1
Aspergillus terreus clone SF_917 small subunit ribosomal RNA gene, partial sequence; internal transcribed spacer 1, 5.8S ribosomal RNA gene, and inte	963	963	100%	0.0	100.00%	MT530193.1
Aspergillus terreus clone SF_915 small subunit ribosomal RNA gene, partial sequence; internal transcribed spacer 1, 5.8S ribosomal RNA gene, and inte	963	963	100%	0.0	100.00%	MT530191.1
Aspergillus terreus clone SF_914 small subunit ribosomal RNA gene, partial sequence; internal transcribed spacer 1, 5.8S ribosomal RNA gene, and inte	963	963	100%	0.0	100.00%	MT530190.1
Aspergillus terreus clone SF_894 small subunit ribosomal RNA gene, partial sequence; internal transcribed spacer 1, 5.8S ribosomal RNA gene, and inte	963	963	100%	0.0	100.00%	MT530170.1

Fig. 12 *Aspergillus terreus (MT558939.1)* isolate 2011F5 small subunit ribosomal RNA gene, partial sequence; internal transcribed spacer 1, 5.8S ribosomal RNA gene, and internal transcribed spacer 2, complete sequence; and large subunit ribosomal RNA gene, partial sequence.

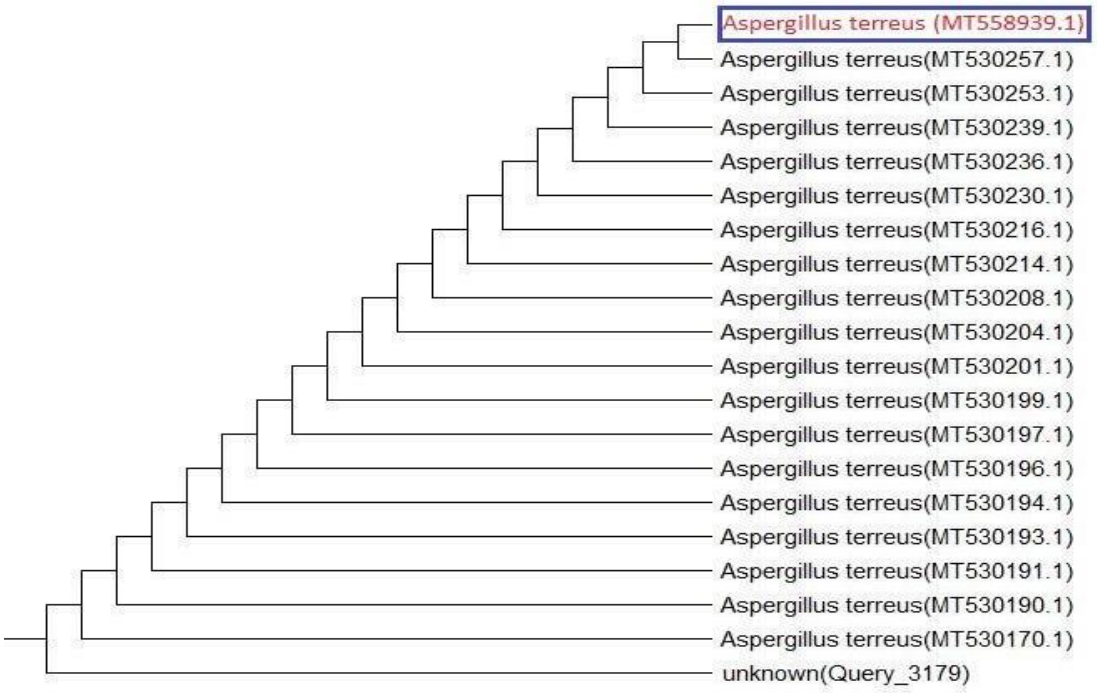

Fig. 13 Phylogenetic tree of *Aspergillus terreus (MT558939.1).*

	Description	Max Score	Total Score	Query Cover	E value	Per. Ident	Accession
☑	Aspergillus sp. isolate MEBP0048 small subunit ribosomal RNA gene, partial sequence; internal transcribed spacer 1, 5.8S ribosomal RNA gene, and inte	948	948	100%	0.0	100.00%	MT645617.1
☑	Aspergillus flavus isolate LUOHE small subunit ribosomal RNA gene, partial sequence; internal transcribed spacer 1, 5.8S ribosomal RNA gene, and inte	948	948	100%	0.0	100.00%	MT645322.1
☑	Aspergillus flavus isolate MT1 small subunit ribosomal RNA gene, partial sequence; internal transcribed spacer 1, 5.8S ribosomal RNA gene, and internal	948	948	100%	0.0	100.00%	MT629885.1
☑	Aspergillus flavus isolate BB-1 small subunit ribosomal RNA gene, partial sequence; internal transcribed spacer 1, 5.8S ribosomal RNA gene, and interna	948	948	100%	0.0	100.00%	MT584825.1
☑	Aspergillus flavus strain RM719 internal transcribed spacer 1, partial sequence; 5.8S ribosomal RNA gene and internal transcribed spacer 2, complete se	948	948	100%	0.0	100.00%	MT584295.1
☑	Aspergillus flavus strain RM272 internal transcribed spacer 1, partial sequence; 5.8S ribosomal RNA gene and internal transcribed spacer 2, complete se	948	948	100%	0.0	100.00%	MT584281.1
☑	Aspergillus oryzae isolate 2011F18 small subunit ribosomal RNA gene, partial sequence; internal transcribed spacer 1, 5.8S ribosomal RNA gene, and int	948	948	100%	0.0	100.00%	MT558944.1
☑	Aspergillus flavus isolate 2011F7 small subunit ribosomal RNA gene, partial sequence; internal transcribed spacer 1, 5.8S ribosomal RNA gene, and inter	948	948	100%	0.0	100.00%	MT558941.1
☑	Aspergillus flavus isolate H internal transcribed spacer 1, partial sequence; 5.8S ribosomal RNA gene and internal transcribed spacer 2, complete sequer	948	948	100%	0.0	100.00%	MT550030.1
☑	Aspergillus flavus isolate RMUAF43 internal transcribed spacer 1, partial sequence; 5.8S ribosomal RNA gene and internal transcribed spacer 2, complet	948	948	100%	0.0	100.00%	MT541873.1
☑	Aspergillus oryzae isolate RMUAO56 internal transcribed spacer 1, partial sequence; 5.8S ribosomal RNA gene and internal transcribed spacer 2, compl	948	948	100%	0.0	100.00%	MT541869.1
☑	Aspergillus flavus clone SF_740 small subunit ribosomal RNA gene, partial sequence; internal transcribed spacer 1, 5.8S ribosomal RNA gene, and interr	948	948	100%	0.0	100.00%	MT530016.1
☑	Aspergillus flavus clone SF_654 internal transcribed spacer 1, partial sequence; 5.8S ribosomal RNA gene and internal transcribed spacer 2, complete se	948	948	100%	0.0	100.00%	MT529930.1
☑	Aspergillus flavus clone SF_595 small subunit ribosomal RNA gene, partial sequence; internal transcribed spacer 1, 5.8S ribosomal RNA gene, and interr	948	948	100%	0.0	100.00%	MT529871.1
☑	Aspergillus flavus clone SF_593 internal transcribed spacer 1, partial sequence; 5.8S ribosomal RNA gene and internal transcribed spacer 2, complete se	948	948	100%	0.0	100.00%	MT529869.1
☑	Aspergillus flavus clone SF_562 small subunit ribosomal RNA gene, partial sequence; internal transcribed spacer 1, 5.8S ribosomal RNA gene, and interr	948	948	100%	0.0	100.00%	MT529838.1
☑	Aspergillus flavus clone SF_544 small subunit ribosomal RNA gene, partial sequence; internal transcribed spacer 1, 5.8S ribosomal RNA gene, and interr	948	948	100%	0.0	100.00%	MT529820.1
☑	Aspergillus flavus clone SF_513 small subunit ribosomal RNA gene, partial sequence; internal transcribed spacer 1, 5.8S ribosomal RNA gene, and interr	948	948	100%	0.0	100.00%	MT529789.1
☑	Aspergillus flavus clone SF_316 small subunit ribosomal RNA gene, partial sequence; internal transcribed spacer 1, 5.8S ribosomal RNA gene, and interr	948	948	100%	0.0	100.00%	MT529592.1
☐	Aspergillus flavus clone SF_124 small subunit ribosomal RNA gene, partial sequence; internal transcribed spacer 1, 5.8S ribosomal RNA gene, and interr	948	948	100%	0.0		
☐	Aspergillus flavus clone SF_118 small subunit ribosomal RNA gene, partial sequence; internal transcribed spacer 1, 5.8S ribosomal RNA gene, and interr	948	948	100%	0.0		

Questions/comm

Fig. 14 *Aspergillus flavus (MT645322.1)* isolate LUOHE small subunit ribosomal RNA gene, partial sequence; internal transcribed spacer 1, 5.8S ribosomal RNA gene, and internal transcribed spacer 2, complete sequence; and large subunit ribosomal RNA gene, partial sequence.

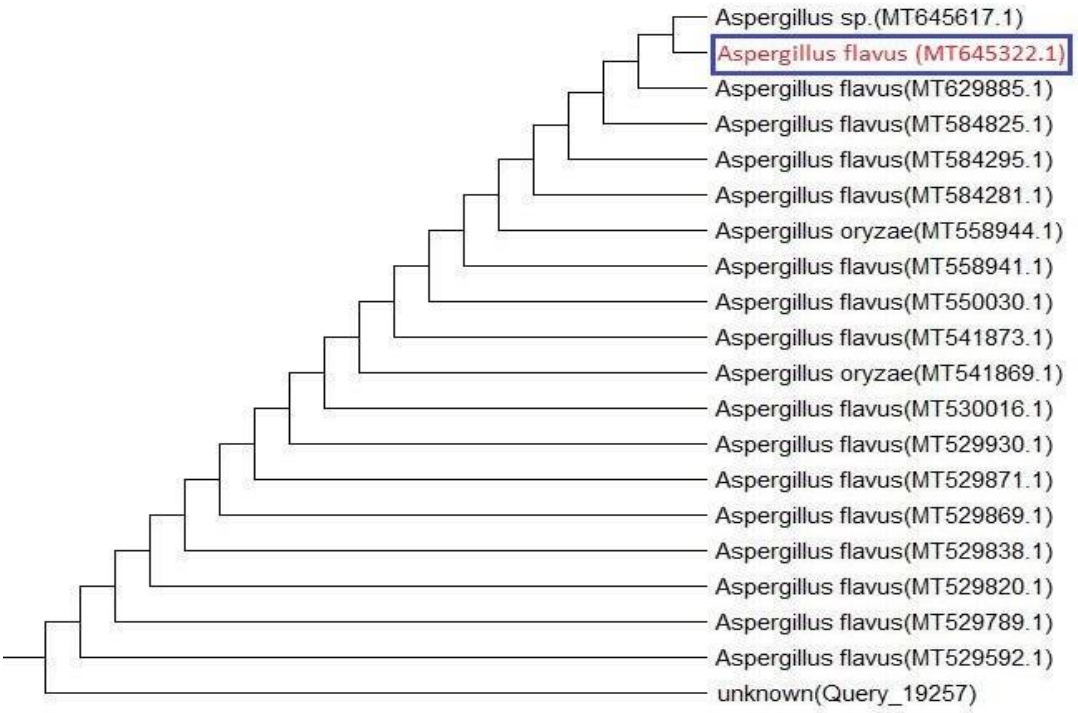

Fig. 15 Phylogenetic tree of *Aspergillus flavus (MT645322.1).*

Description	Max Score	Total Score	Query Cover	E value	Per. Ident	Accession
Bacillus paramycoides strain MCCC 1A04098 16S ribosomal RNA, partial sequence	1397	1397	100%	0.0	99.74%	NR_157734.1
Bacillus tropicus strain MCCC 1A01406 16S ribosomal RNA, partial sequence	1391	1391	100%	0.0	99.61%	NR_157736.1
Bacillus nitratireducens strain MCCC 1A00732 16S ribosomal RNA, partial sequence	1391	1391	100%	0.0	99.61%	NR_157732.1
Bacillus luti strain MCCC 1A00359 16S ribosomal RNA, partial sequence	1391	1391	100%	0.0	99.61%	NR_157730.1
Bacillus albus strain MCCC 1A02146 16S ribosomal RNA, partial sequence	1391	1391	100%	0.0	99.61%	NR_157729.1
Bacillus cereus strain IAM 12605 16S ribosomal RNA, partial sequence	1386	1386	100%	0.0	99.48%	NR_115526.1
Bacillus thuringiensis strain IAM 12077 16S ribosomal RNA, partial sequence	1386	1386	100%	0.0	99.48%	NR_043403.1
Bacillus wiedmannii strain FSL W8-0169 16S ribosomal RNA, partial sequence	1386	1386	100%	0.0	99.48%	NR_152692.1
Bacillus proteolyticus strain MCCC 1A00365 16S ribosomal RNA, partial sequence	1386	1386	100%	0.0	99.48%	NR_157735.1
Bacillus pacificus strain MCCC 1A06182 16S ribosomal RNA, partial sequence	1386	1386	100%	0.0	99.48%	NR_157733.1
Bacillus mobilis strain MCCC 1A05942 16S ribosomal RNA, partial sequence	1386	1386	100%	0.0	99.48%	NR_157731.1
Bacillus paranthracis strain MCCC 1A00395 16S ribosomal RNA, partial sequence	1386	1386	100%	0.0	99.48%	NR_157728.1
Bacillus fungorum strain 17-SMS-01 16S ribosomal RNA, partial sequence	1386	1386	100%	0.0	99.48%	NR_170494.1
Bacillus cereus ATCC 14579 16S ribosomal RNA (rrnA), partial sequence	1386	1386	100%	0.0	99.48%	NR_074540.1
Bacillus toyonensis strain BCT-7112 16S ribosomal RNA, partial sequence	1386	1386	100%	0.0	99.48%	NR_121761.1
Bacillus cereus strain CCM 2010 16S ribosomal RNA, partial sequence	1386	1386	100%	0.0	99.48%	NR_115714.1
Bacillus cereus strain NBRC 15305 16S ribosomal RNA, partial sequence	1386	1386	100%	0.0	99.48%	NR_112630.1
Bacillus cereus ATCC 14579 16S ribosomal RNA, partial sequence	1386	1386	100%	0.0	99.48%	NR_114582.1
Bacillus thuringiensis strain ATCC 10792 16S ribosomal RNA, partial sequence	1386	1386	100%	0.0	99.48%	NR_114581.1

Fig. 16 *Bacillus paramycoides* strain MCCC 1A04098 16S ribosomal RNA, partial sequence.

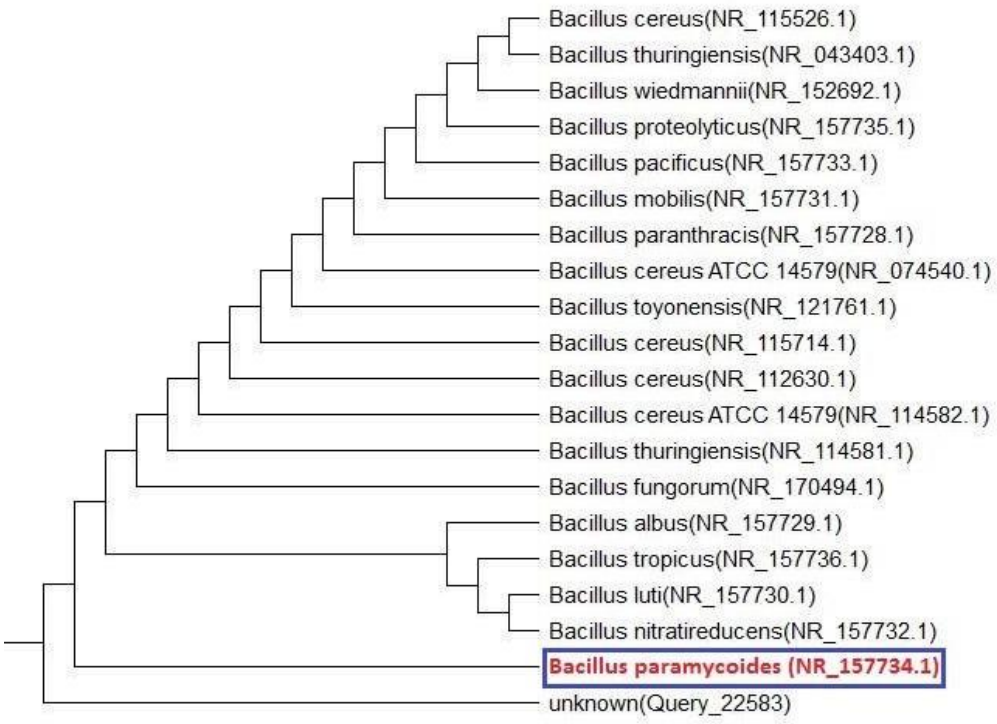

Fig. 17 Phylogenetic tree of *Bacillus paramycoides (NR_157734.1).*

Description	Max Score	Total Score	Query Cover	E value	Per. Ident	Accession
Bacillus subtilis subsp. spizizenii strain NRRL B-23049 16S ribosomal RNA, partial sequence	1070	1070	97%	0.0	99.16%	NR_024931.1
Bacillus subtilis subsp. spizizenii strain NBRC 101239 16S ribosomal RNA, partial sequence	1070	1070	97%	0.0	99.16%	NR_112686.1
Bacillus subtilis subsp. inaquosorum strain BGSC 3A28 16S ribosomal RNA, partial sequence	1064	1064	97%	0.0	98.99%	NR_104873.1
Bacillus mojavensis strain ifo 15718 16S ribosomal RNA, partial sequence	1064	1064	97%	0.0	98.99%	NR_118290.1
Bacillus halotolerans strain CR-95 16S ribosomal RNA, partial sequence	1064	1064	97%	0.0	98.99%	NR_115282.1
Bacillus halotolerans strain LMG 22477 16S ribosomal RNA, partial sequence	1064	1064	97%	0.0	98.99%	NR_115931.1
Bacillus halotolerans strain CECT 5687 16S ribosomal RNA, partial sequence	1064	1064	97%	0.0	98.99%	NR_115930.1
Bacillus halotolerans strain LMG 22476 16S ribosomal RNA, partial sequence	1064	1064	97%	0.0	98.99%	NR_115929.1
Bacillus halotolerans strain DSM 8802 16S ribosomal RNA, partial sequence	1064	1064	97%	0.0	98.99%	NR_115063.1
Bacillus tequilensis strain 10b 16S ribosomal RNA, partial sequence	1064	1064	97%	0.0	98.99%	NR_104919.1
Bacillus subtilis strain DSM 10 16S ribosomal RNA, partial sequence	1059	1059	97%	0.0	98.82%	NR_027552.1
Bacillus subtilis strain IAM 12118 16S ribosomal RNA, complete sequence	1059	1059	97%	0.0	98.82%	NR_112116.2
Bacillus mojavensis strain IFO15718 16S ribosomal RNA, partial sequence	1059	1059	97%	0.0	98.82%	NR_024693.1
Bacillus subtilis strain BCRC 10255 16S ribosomal RNA, partial sequence	1059	1059	97%	0.0	98.82%	NR_116017.1
Bacillus subtilis strain JCM 1465 16S ribosomal RNA, partial sequence	1059	1059	97%	0.0	98.82%	NR_113265.1
Bacillus mojavensis strain NBRC 15718 16S ribosomal RNA, partial sequence	1059	1059	97%	0.0	98.82%	NR_112725.1
Bacillus subtilis strain NBRC 13719 16S ribosomal RNA, partial sequence	1059	1059	97%	0.0	98.82%	NR_112629.1
Bacillus halotolerans strain CR-119 16S ribosomal RNA, partial sequence	1055	1055	97%	0.0	98.66%	NR_115283.1
Bacillus vallismortis strain NBRC 101236 16S ribosomal RNA, partial sequence	1055	1055	97%	0.0	98.66%	NR_113994.1

Fig. 18 *Bacillus subtilis subsp. spizizenii* strain NRRL B-23049 16S ribosomal RNA, partial sequence.

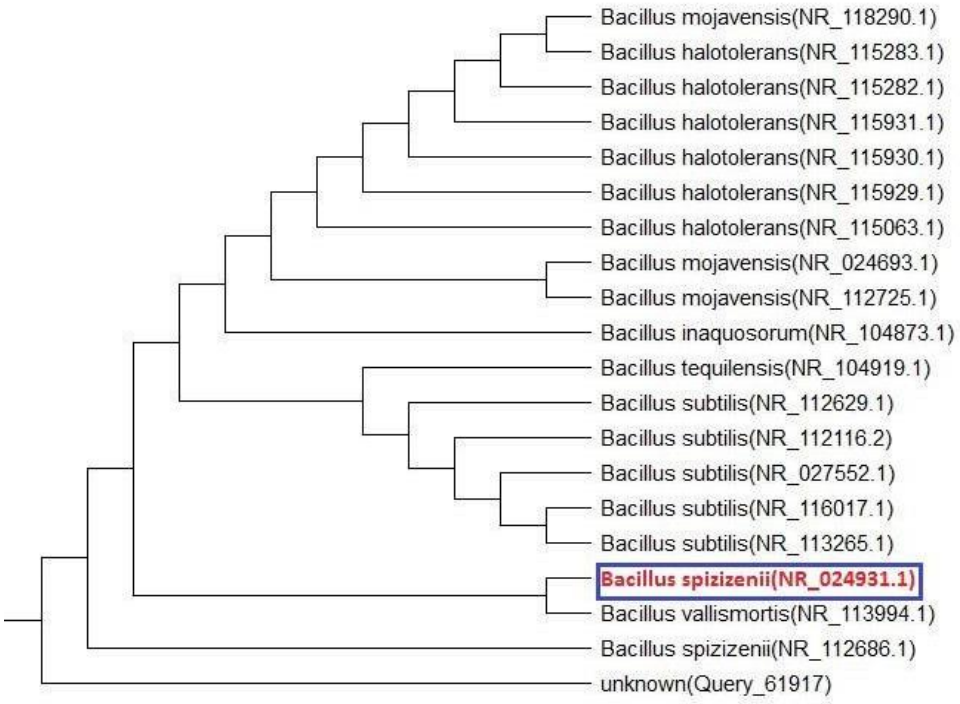

Fig.19 Phylogenetic tree of *Bacillus subtilis spizizenii (NR_024931.1).*

Description	Max Score	Total Score	Query Cover	E value	Per. Ident	Accession
Enterobacter cancerogenus strain LMG 2693 16S ribosomal RNA, partial sequence	1129	1129	100%	0.0	99.04%	NR_044977.1
Enterobacter cancerogenus strain LMG 2693 16S ribosomal RNA, partial sequence	1129	1129	100%	0.0	99.04%	NR_116756.1
Cedecea lapagei strain DSM 4587 16S ribosomal RNA, partial sequence	1127	1127	100%	0.0	99.04%	NR_126318.1
Enterobacter ludwigii strain EN-119 16S ribosomal RNA, partial sequence	1127	1127	100%	0.0	99.04%	NR_042349.1
Pantoea agglomerans strain JCM1236 16S ribosomal RNA, partial sequence	1122	1122	100%	0.0	98.89%	NR_111998.1
Enterobacter hormaechei subsp. xiangfangensis strain 10-17 16S ribosomal RNA, partial sequence	1122	1122	100%	0.0	98.89%	NR_126208.1
Enterobacter mori LMG 25706 strain R18-2 16S ribosomal RNA, partial sequence	1116	1116	100%	0.0	98.73%	NR_116430.1
Enterobacter bugandensis strain 247BMC 16S ribosomal RNA, partial sequence	1112	1112	100%	0.0	98.57%	NR_148649.1
Klebsiella aerogenes strain ATCC 13048 16S ribosomal RNA, partial sequence	1110	1110	100%	0.0	98.57%	NR_118556.1
Citrobacter murliniae strain CDC 2970-59 16S ribosomal RNA, partial sequence	1110	1110	100%	0.0	98.57%	NR_028688.1
Citrobacter braakii strain 167 16S ribosomal RNA, partial sequence	1110	1110	100%	0.0	98.57%	NR_028687.1
Klebsiella aerogenes KCTC 2190 16S ribosomal RNA, complete sequence	1110	1110	100%	0.0	98.57%	NR_102493.2
Klebsiella aerogenes strain JCM 1235 16S ribosomal RNA, partial sequence	1110	1110	100%	0.0	98.57%	NR_024643.1
Enterobacter asburiae strain JCM6051 16S ribosomal RNA, partial sequence	1110	1110	100%	0.0	98.57%	NR_024640.1
Citrobacter cronae strain Tue2_1 16S ribosomal RNA, partial sequence	1110	1110	100%	0.0	98.57%	NR_170426.1
Enterobacter hormaechei strain 0992-77 16S ribosomal RNA, partial sequence	1107	1107	100%	0.0	98.41%	NR_042154.1
Leclercia adecarboxylata strain NBRC 102595 16S ribosomal RNA, partial sequence	1107	1107	100%	0.0	98.41%	NR_114154.1
Klebsiella aerogenes strain NBRC 13534 16S ribosomal RNA, partial sequence	1107	1107	100%	0.0	98.41%	NR_113614.1
Leclercia adecarboxylata strain CIP 82.92 16S ribosomal RNA, partial sequence	1105	1105	100%	0.0	98.41%	NR_104933.1

Fig. 20 *Enterobacter cancerogenus* strain LMG 2693 16S ribosomal RNA, partial sequence.

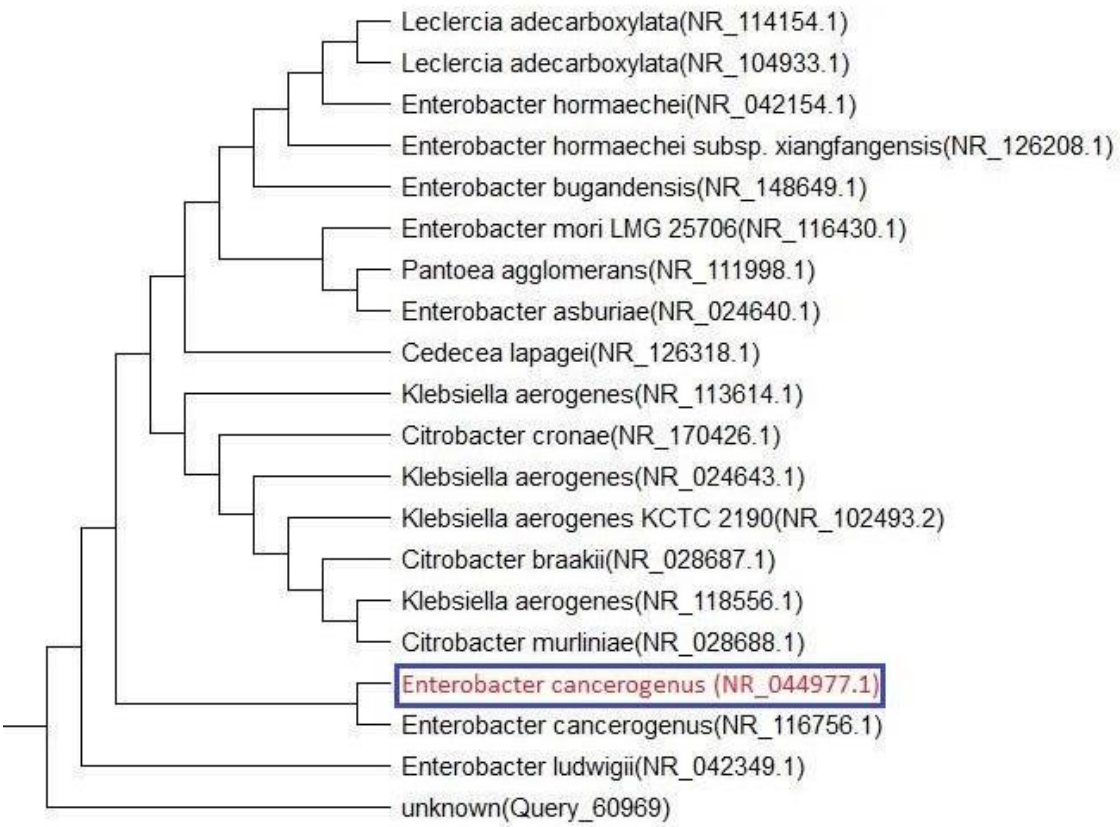

Fig. 21 Phylogenetic tree of *Enterobacter cancerogenus (NR_044977.1).*

شركة سيجما للخدمات العلمية
Sigma Scientific Services Co.

Sigma Scientific Services Co.

افاده

نحيط علم حضراتكم بان الشركه قد قامت بعمل تعريف لعينات بكتريا و
فطريات خاصه بدكتوره ناهد فريد عن طريق تحليل
(DNA Sequencing)

وذلك بناء علي طلب من الباحث ورغبته بأرسال العينات عن طريق شركتنا

ولكم جزيل الشكر

سيجما للخدمات
العلمية

Head Office: : Lebon building- La Cite mall - El Hossary - 6 of October, Cairo - Egypt.
Tel. 0233451883 - Fax02 33451883 - +2 0168845349 E - mail Sigmas.s@Hotmail.com

Fig. 22 Sigma scientific services report.

Table 1. GCMS of *Aspergillus flavus (MT645322.1)*

RT	Compound Name For *Aspergillus flavus (MT645322.1)* bioactive	Formula	MW	Area %
12.48	1,10-Decanediol monotetrahydro-2-pyranyl ether	C15H30O3,	258	0.51
13.6	2,4-Di-tert-butylphenol	C14H22O,	206	2.97
15.64	HEXADECAN-1-OL	C16H34O,	242	0.72
17.06	Oxalic acid, dodecyl 3,5-difluorophenyl ester	C20H28F2O4,	370	2.78
17.42	3-(2-HYDROXY-4,4-DIMETHYL-6-OXO-1-CYCLOHEXEN-1-YL)-4-OXOPENTANOIC ACID	C13H18O5,	254	0.45
18.69	Dimethyl myristamine	C16H35N,	241	6.46
18.99	DODECAN-5-ONE	C12H24O,	184	0.48
19.79	Hexa-hydro-farnesol	C15H32O,	228	0.62
21.01	(9E)-9-Hexadecen-1-ol	C16H32O,	240	4.38
21.1	Erythro-9,10-dihydroxyoctadecanoic	C18H36O4,	316	1.36
21.62	Pyrrolo[1,2-a]pyrazine-1,4-dione,hexahydro-3-(2-methylpropyl)-	C11H18N2O2,	210	5.68
21.88	5-(1-Hydroxypentyl)-3,3a,4,6a-tetrahydro-2H-cyclopenta[b]furan-2-one	C12H18O3,	210	0.37
22.9	Phen-1,4-diol	C9H9F3O2	206	0.51

23.5	Pent-4-enoic acid, 2-(2-hydroxy-3-isobutoxypropyl)-, hydrazide	C12H24N2O3,	244	31.19
23.8	Decan-2-yl isobutyl carbonate	C15H30O3,	258	6.29
24	2-CYCLOHEXEN-1-ONE, 2-HYDROXY-3,5,5-TRIMETHYL	C9H14O2,	154	0.93
24.2	7,9-Di-tert-butyl-1-oxaspiro(4,5)deca-6,9-diene-2,8-dione	C17H24O3,	276	0.51
24.69	PENTADECANOIC ACID, 14-METHYL-, METHYL ESTER	C17H34O2,	270	0.49
25.99	1-Eicosanol	C20H42O,	280	9.15
28.33	8,11-OCTADECADIENOIC ACID, METHYL ESTER	C19H34O2,	294	0.50
28.48	Oleic acid, methyl ester	C19H36O2,	296	0.99
28.68	Ethylenediamine, N,N'-dibenzyl-N,N'-dimethyl-	C18H24N2	268	3.73
29.11	OCTADECANOIC ACID, METHYL ESTER	C19H38O2,	298	0.51
30.57	1-Docosene	C22H44,	308	7.37
33.22	N-Methyl-N-benzyltetradecanamine	C22H39N	317	0.96
34.3	3,4',5,6'-tetra-tert-butylbiphenyl-2,3'-diol	C28H42O2,	410	0.62
34.79	Nonacos-1-ene	C29H58,	406	3.75
37.79	3',8,8'-Trimethoxy-3-piperidyl-2,2'-binaphthalene-1,1',4,4'-tetrone	C28H25NO7	487	0.37
38.69	Nonacos-1-ene	C29H58	406	1.70
42.39	2-METHYLHEXADECAN-1-OL	C17H36O,	256	0.65
42.79	Cholestan-3-ol, 2-methylene-, (3á,5à)-	C28H48O,	400	0.29
43.9	9,12-OCTADECADIENOIC ACID (Z,Z)-, 2,3-BIS[(TRIMETHYLSILYL)OXY]PROPYL ESTER	C27H54O4Si2,	498	0.38
44.18	3',4',7-TRIMETHYLQUERCETIN	C18H16O7,	344	0.36
44.38	9,10-SECOCHOLESTA-5,7,10(19)-TRIENE-3,24,25-TRIOL, (3á,5Z,7E)-	C27H44O3,	416	1.97

Table 2. GCMS of *Aspergillus fumigatus (MT635279.1)*

RT	**Compound Name For *Aspergillus fumigatus (MT635279.1)* bioactive**	**Formula**	**MW**	**Area %**
5.31	(3Z)-3-Dodecene	C12H24	168	1.16
10.08	7-Tetradecene	C14H28,	196	0.86
10.18	7-HEXADECENE, (Z)-	C16H32,	224	2.2
11.82	9-Octadecen-12-ynoic acid, methyl ester	C19H32O2,	292	2.73
13.27	1-DIMETHYLAMINODODECANE	C14H31N,	213	8.04
13.6	2,4-DITERT-BUTYLPHENOL	C14H22O,	206	3.27
15.14	7,9-Di-tert-butyl-1-oxaspiro(4,5)deca-6,9-diene-2,8-dione	C17H24O3,	276	1.25
15.65	(3E)-3-Tetradecene	C14H28,	196	4.56
16.26	cis-Z-à-Bisabolene epoxide	C15H24O,	220	0.64
16.68	3a,9-Dimethyldodecahydrocyclohepta[d]inden-3-one	C16H26O,	234	1.07
18.42	5-Caranol, trans,trans-(+)-	C10H18O,	154	0.56
18.69	N,N-DIMETHYL-1-TETRADECANAMINE	C16H35N	241	3.55
19.37	7,10,13-Hexadecatrienoic acid, methyl	C17H28O2,	264	0.97
21.01	1-Nonadecene	C19H38,	266	6.48
21.59	Pyrrolo[1,2-a]pyrazine-1,4-dione, hexahydro-3-(2-methylpropyl)-	C11H18N2O2,	210	1.68
22.3	CARYOPHYLLENOXID	C15H24O,	220	1.2
22.71	5-Heptenoic acid, 6-methyl-4-[(4-methylphenyl) sulfonyl]	C15H20O4S,	296	0.54
22.93	Phen-1,4-diol, 2,3-dimethyl-5-trifluoromethyl-	C9H9F3O2,	206	1.35
23.16	Isoaromadendrene	C15H24O,	220	2.22
23.44	9-t-Butyltricyclo[4.2.1.1(2,5)]decane-9,10-diol	C14H24O2,	224	1.4
24	5-Ethenyl-5-(1-methyl-3-butenyl)-hexahydropyrimidine-2,4,6-trione	C11H14N2O3,	222	1.7
24.4	Palmitic acid, methyl ester	C17H34O2,	270	0.9
24.5	3,7-Diazabicyclo[3.3.1]nonane, 9,9-dimethyl-	C9H18N2,	154	4.71

25.99	1-Eicosanol	C20H42O,	298	8.06
27.38	E,E,Z-1,3,12-Nonadecatriene-5,14-diol	C19H34O2,	294	1.03
28.33	12-Methyl-E,E-2,13-octadecadien-1-ol	C19H36O,	280	0.69
28.48	cis-Vaccenic acid	C18H34O2,	282	0.93
28.69	N-Methyl-N-benzyltetradecanamine	C22H39N	317	1.96
30.57	1-Nonacosene	C29H58,	406	6.35
32.82	1-Hexadecanol, 2-methyl-	C17H36O,	256	0.79
33.23	1-CHLOROOCTADECANE	C18H37Cl,	288	0.58
34.31	Octadecane, 3-ethyl-5-(2-ethylbutyl)-	C26H54,	366	1.28
34.8	DOCOSAN-1-OL	C22H46O,	326	4.17
37.79	5-ACETOXY-6-METHYL-12,13-DIOXA-TRICYCLO[7.3.1.0 1,6]TRIDECANE-10-CARBOXYLIC ACID	C15H22O6,	298	1.48
38.7	1-HEPTACOSANOL	C27H56O,	396	1.61
41.36	Prostaglandin A1-biotin	C35H58N4O5S	646	1.51
41.85	6-METHOXY-13H-[1,3]DIOXOLO[7,8][1]BENZOXEPINO[2,3,4-IJ]ISOQUINOLINE	C18H13NO4,	307	9.51
42.4	Erucic acid	C22H42O2,	338	0.88
43.9	3',4',7-TRIMETHYLQUERCETIN	C18H16O7,	344	0.8
44.18	(Z,Z)-1,3-DIOCTADECENOYL GLYCEROL	C39H72O5,	620	0.58
44.38	Ethyl iso-allocholate	C26H44O5	436	1.11
44.74	9,10-SECOCHOLESTA-5,7,10(19)-TRIENE-3,24,25-TRIOL, (3á,5Z,7E)-	C27H44O3,	416	3.64

Table 3. GCMS of *Aspergillus terreus (MT558939.1)*

RT	**Compound Name For *Aspergillus terreus (MT558939.1)* bioactive**	**Formula**	**MW**	**AREA %**
6.81	3-t-Pentylcyclopentanone	C10H18O,	154	10.1
9.51	Nerol acetate	C12H20O2,	196	1.6
10.03	(R)-lavandulyl acetate	C12H20O2,	196	1.4
13.26	1-DODECANAMINE, N,N-DIMETHYL	C14H31N,	213	6.5
13.59	BUTYLHYDROQUINONE	C13H18O2,	206	2.5
15.63	n-Cetyl alcohol	C16H34O,	242	1.4
18.7	1-TETRADECANAMINE, N,N-DIMETHYL	C16H35N,	241	16.4
21	1-Eicosanol	C20H42O,	298	4.7
21.58	3-(Hydroxymethyl)-5-methoxyphenol	C8H10O3,	154	2.6
22.05	DI-AMYLCYCLOHEXANO	C16H32O,	240	0.9
22.73	4,4,8-TRIMETHYL-TRICYCLO[6.3.1.0 1,5]DODECANE-2,9-DIOL	C15H26O2,	238	0.7
23.16	p-Menth-8-en-3-ol, acetate	C12H20O2,	196	1.1
23.99	Pyrrolo[1,2-a]pyrazine-1,4-dione, hexahydro-3-(2-methylpropyl)-	C11H18N2O2,	210	1.0
24.17	7,9-Di-tert-butyl-1-oxaspiro(4,5)deca-6,9-diene-2,8-dione	C17H24O3,	276	0.4
24.38	Palmitic acid, methyl ester	C17H34O2,	270	1.4
24.49	3,7-Diazabicyclo[3.3.1]nonane, 9,9-dimethyl-	C9H18N2,	154	1.6
25.45	Oleic Acid	C18H34O2,	282	1.3
25.98	1-Nonadecene	C19H38	266	8.5
26.26	Labd-7-en-15-oic acid	C20H34O2,	306	0.5

27.8	[4-(Thiophen-3-yl)oxan-4-yl]methanol	C10H14O2S,	198	3.4
28.32	Methyl 9-cis,11-trans-octadecadienoate	C19H34O2,	294	1.2
28.47	Oleic acid, methyl ester	C19H36O2,	296	1.1
28.68	N-Methyl-N-benzyltetradecanamine	C22H39N,	317	1.1
29.11	16-Octadecenoic acid, methyl ester	C19H36O2,	296	1.0
29.52	trans-13-Octadecenoic acid	C18H34O2,	282	0.8
29.64	(9E,12E)-9,12-OCTADECADIENOYL CHLORIDE	C18H31ClO,	298	0.5
30.56	n-Eicosanol	C20H42O,	298	7.3
34.29	3,4',5,6'-tetra-tert-butylbiphenyl-2,3'-diol	C28H42O2,	410	0.9
34.78	1-Docosene	C22H44,	308	3.7
35.49	i-Propyl 5,9,17-hexacosatrienoate	C29H52O2,	432	0.7
37.42	Chromone, 5-hydroxy-6,7,8-trimethoxy-2,3-dimethyl-	C14H16O6,	280	4.6
37.94	2-PENTANONE, 3,4-DIMETHYL-, (2,4-DINITROPHENYL)HYDRAZONE	C13H18N4O4,	294	2.9
38.19	D:A-Friedooleanan-3-ol, (3à)-	C30H52O,	428	0.7
38.69	2-METHYLHEXADECAN-1-OL	C17H36O,	256	1.8
42.38	17-Pentatriacontene	C35H70	490	0.7
43.93	3',4',7-TRIMETHYLQUERCETIN	C18H16O7,	344	0.9
44.73	(5Z,7E)-9,10-SECOCHOLESTA-5,7,10-TRIENE-3,24,25-TRIOL	C27H44O3,	416	1.9

Table 4. Comparison between *Aspergillus terreus, Aspergillus flavus* and *Aspergillus fumigatus* IC_{50} values compared with that of *Penicillium sp.* against treated A549, HepG2 and MCF7.

IC_{50} µg/ ml	***Aspergillus terreus (MT558939.1)***	***Aspergillus flavus (MT645322.1)***	***Aspergillus fumigatus (MT635279.1)***	**ANOVA**	**p-value**
A549	485aA±17	400bB±16	195cC±13	466.912	<0.001**
HEPG2	235cB±13	1562aA±22	346bB±15	259.413	<0.001**
MCF7	114cC±12	457bB±16	1149aA±19	478.771	<0.001**

*Using: One Way Analysis of Variance; **p-value <0.001 HS*

Different small letters indicate significant difference at (p<0.05) among means in the same row and different capital letter indicates significant difference at (p<0.05) among means in the same column

Table 5. GCMS of *Bacillus paramycoides (NR_157734.1)*

RT	***Compound Name For Bacillus paramycoides (NR_157734.1)***	**Formula**	**MW**	**Area %**
9.52	Nerol acetate	C12H20O2,	196	25.82
13.27	Dodecylamine, N,N-dimethyl-	C14H31N,	213	11.13
28.48	Methyl 10-octadecenoate	C19H36O2	296	3.85
37.8	9-(2',2'-Dimethylpropanoilhydrazono)-3,6-dichloro-2,7-bis-[2-(diethylamino)-ethoxy]fluorine	C30H42Cl2N4O3	576	3.94
41.36	Prostaglandin A1-biotin	C35H58N4O5S	646	22.96
44.74	3',4',7-TRIMETHYLQUERCETIN	C18H16O7,	344	32.3

Table 6. Comparison between *Bacillus paramycoides, Bacillus subtilis spizizenii*, and *Enterobacter cancerogenus* treated A549, HepG2 and MCF7

IC_{50} µg/ ml	***Bacillus paramycoides (NR_157734.1)***	***Bacillus subtilis spizizenii (NR_024931.1)***	***Enterobacter cancerogenus (NR_044977.1)***	**ANOVA**	**p-value**
A5490	1445cA±23	3571aA±42	1602bA±24	338.346	<0.001**
HepG2	428cC±14	1838aC±27	893bC±18	199.66	<0.001**
MCF7	1060cB±20	2385aB±31	1260bB±21	247.017	<0.001**

*Using: One Way Analysis of Variance; **p-value <0.001 HS*

Differences in means among rows denoted by different small letters and differences between means within the same column denoted by different capital letters denote differences between the two groups at the p<0.05 level.

8. References

1. **Deepti Diwan, Lei Cheng, Zeba Usmani, Minaxi Sharma, Nicola Holden, Nicholas Willoughby, Neelam Sangwan, Rama Raju Baadhe, Chenchen Liu, Vijai Kumar Gupta (2021).** Microbial cancer therapeutics: A promising approach. Please cite this article as: Deepti Diwan, Seminars in Cancer Biology https://doi.org/10.1016/j.semcancer.2021.05.003.
2. **Saadia M. Easa, Heba G. Hussein, El-Sayed R. El-Sayed, Nahed A. Younis and Abd El Hamid A. Hamdy. (2022).** Harnessing Endophytic Fungi for Biosynthesis of selenium Nanoparticles and Exploring their Antifungal, Antibacterial and Antioxidant Activities". Applied Microbiology and Biotechnology **EMID: 971 cea 96834 d 5e 66.**
3. **Saadia M. Easa, Hanan M. Abo-Stait, Fatma A Abu Zahra, Amira A. Hassan and Abdel-Mohsen S. Ismail. (2021).** Biosynthesis and Characterization of a novel *Penicillium janthinellum biourge* L asparaginase as a diverse biological activity agent". Egyptian Pharmaceutical Journal, Published by Wolteers Kluwer, Medknov **Doi: 10.4103/epj. Epi-3-21.**
4. **Saadia M. Easa, Saif M. Dmour, N.A. Eltahawy, S.M. Elsonbaty and N.H. Qaralleh (2020).** Ionizing Radiation effect on *Teucrium Poliumi* phytochemical contents antioxidant and antibacterial activity". The Egyptian Society of Nuclear Science and Applications (ESNSA). **ISSN: 1110-0451.**
5. **Saadia M. Easa, Sara M. El-Sousy, Amira A. Hassan and Abdel-Mohsen S. Ismail. (2021).** Biochemical studies on Microbial L- Glutaminase and its Applications. Egyptian Pharmaceutical Journal, Published by Wolteers Kluwer, Medknow; **Doi: 10.4103/epj. Epi-3-21.**
6. **Saadia M. Easa, Mohamed S. Badr and Mohamed Salaheldin. (2022).** Characterization of White Button Mushroom and Its Biomedical Applications Egypt. Acad. J. Biology. **Sci; 14(1): 107-119. ISSN 2090-0767.**
7. **Ashish Bedi, Alok Adholeya and Sunil Kumar Deshmukh. (2017).** Novel Anticancer Compounds from Endophytic Fungi. Current biotechnology volume **6. No.1**

8. **Saadia M. Easa, Al-Shaymaa Abdel-Monaem, Seham Abdel Shafik, Ali Osman and Mohammed F. Ibrahim. (2019).** Inhibition of *Staphylococcus pasteuri* using Moringa aliferea Leaves Extract. Global Scientific Journals, **Volume 7. Issue 9, ISSN: 2320-9186.**
9. **Chakrabhavi Dhananjaya Mohan. (2021). Seminars in Cancer Biology, https://doi.org/10.1016/j.semcancer.2021.05.006**
10. **Saadia M. Easa, Eman Elmansy, Fawkia M. El-Beih, Ebtsam M. El-Kady and Mohsen S. Asker. (2017).** Optimization, Production, and Partial Purification of Thermostable α- Amylase Produced by Marine Bacterium *Bacillus sp. NRC 12017*, International Journal of Pharmaceutical and Clinical Research 2017; **9(8): 558-570, doi: 10.25258/ijpcr. V9i08.958, ISSN-0975 1556.**
11. **Yi He, Bin Wangd, Wanping Chene, Russell J. Coxf, Jingren Hea, Fusheng Chene. (2018).** Recent advances in reconstructing microbial secondary metabolites biosynthesis in Aspergillus **spp. 0734-9750.**
12. **Saadia M. Easa, Hagar M. Abd-El Rahman, Fawkia El Beih and Samar Samir Mohamed. (2021).** Epidemiology and control of nosocomial Pathogens recovered from some Governmental hospitals, Cairo, Egypt, Egyptian Journal of Microbiology Mannscrippt **ID: EJM. 2104-1195.**
13. **Jing Ke, David Robinson, Zong Yen Wu, Andrea Kuftin, Katherine Louie, Suzanne Kosina, Trent Northen, Jan Fang Cheng and Yasuo Yoshikuni. (2022).** Facilitates rapid activation of secondary metabolite biosynthetic gene clusters in bacteria. Cell Chemical Biology **29**, **1–15**, March **17**, **2022**. Cell Chemical Biology **(2021)**, **https://doi.org/10.1016/j.chembiol.2021.08.009**
14. **Saadia M. Easa, Dina Elkahky, Magdy Attia, Nemate M. Awad and Eman A. Helmy. (2019).** Biosynthesis of zinc oxide nanoparticles using *Aspergillus terreus* and their applications as antitumor and antimicrobial activity" Global Advanced Research j. of Agricultural Science **8 (3) (ISSN: 2315-5094).**
15. **Saadia M. Easa, Mattar Z.A, Khalaf, M.A. and Khalil; M.F.A. (2021).** Biosynthesis of Lovastatin by Gamma Irradiated *Aspergillus terreus* J. Nucl. Tech. Appl. Soi; **vol; 9, pp. 19-31. DOI: 10.216808/jntas. 2021.54135.36.1031.**
16. **Saadia M. Easa, Maysa E. Mohran, Magda A. El-Bendary, Fawkia El-Beih, Mostafa M. Abo Elsoud Mohamed I. Azzam Nora N. Elgammal. (2019).** Optimization of fibrinolytic enzyme production by newly isolated *Bacilllus subtilis Egy*. Using central composite design Biocatalysis and Agricultural Biotechnology. **Volume 17, January 2019, Pages 43-50**
17. **Saadia M. Easa, Noura N. Elgamal, Fawkia El-Beih, Maysa Moharan, Magda A. El-Bendary and Mostafa Abo Elsoud. (2018).** Purification of characterization of fibrinolytic enzyme produced by *Bacillus subtilis Egy.* Egypt. Acad. J. Biolog. **Sci, 10 (1): 89-98 (ISSN: 2090-0872).**
18. **Shiyu Song, Miza S. Vuai and Mintao Zhong. (2018).** The role of bacteria in cancer therapy enemies in the past, but allies at present.
19. **Buclin, T., Thoma, Y., Widmer, N., André, P., Guidi, M., Csajka, C., & Decosterd, L. A. (2020).** The steps to therapeutic drug monitoring: a structured approach illustrated with imatinib. Frontiers in Pharmacology, **11, 177.**
20. **Li, C., & Han, X. (2020).** Melanoma cancer immunotherapy using PD-L1 siRNA and imatinib promotes cancer-immunity cycle. Pharmaceutical Research, **37(6), 1-10.**

21. **Yao, Z., Zhang, J., Zhang, B., Liang, G., Chen, X., Yao, F., & Yang, B. (2018).** Imatinib prevents lung cancer metastasis by inhibiting M2-like polarization of macrophages. Pharmacological research, **133, 121-131.**
22. **Bhardwaj A, Sharma D, Jodan N, Agrawal PK. (2015).** Antimicrobial and phytochemical screening of endophytic fungi isolated from spikes of *Pinus rouxburghii*. Arch Clin Microbiol.;**6(3):1.**
23. **Daniel C. Moreira (2022).** RGBradford: Accurate measurement of protein concentration using a smartphone camera and the blue to green intensity ratio. Analytical Biochemistry **Volume 655, 15 October 2022, 114839.**
24. **Jyoti Goutam, Gunjan Sharma, Vinod K. Tiwari, Amrita Mishra, Ravindra N. Kharwar, Vijayakumar Ramaraj and Biplob Koch (2017).** Isolation and Characterization of "Terrein" an Antimicrobial and Antitumor Compound from Endophytic Fungus *Aspergillus terreus* (JAS-2) Associated from Achyranthus aspera Varanasi, India Frontiers in Microbiology | www.frontiersin.org **July 2017 | Volume 8 | Article 1334.**
25. **Zhao, L. Zhou, J. Wang, T. Shan, L. Zhong, X. Liu, and X. GAO. (2010):** Endophytic Fungi for producing bioactive compounds originally from their host plants.
26. **Dimri, M., & Satyanarayana, A. (2020).** Molecular signaling pathways and therapeutic targets in hepatocellular carcinoma. Cancers, **12(2), 491.**
27. **Matthew C. B. Tsilimigras, Anthony Fodorand, Christian Jobin (2017).** Carcinogenesis and therapeutics: the microbiota perspective. **Volume: 2 Article number: 17008.**
28. **Bhatt, K., Agolli, A., Patel, M. H., Garimella, R., Devi, M., Garcia, E., & Sanchez-Gonzalez, M. (2021).** High mortality co-infections of COVID-19 patients: mucormycosis and other fungal infections. Discoveries**, 9(1).**
29. **Gaspar P. Pinto, Natalie M. Hendrikse, Jan Stourac, Jiri Damborsky, David Bednar. (2021).** Virtual screening of potential anticancer drugs based on microbial products.
30. **Mann, A., Rana, J. S., Gaurav, S., & Nehra, K. (2022).** Complete genome analysis of multi drug resistant *Klebsiella aerogenes* for detection of antibiotic resistance genes in bacterial isolates prevalent in agricultural soils.
31. **Laurence Zitvogel1, Romain Daillère, María Paula Roberti1, Bertrand Routy and Guido Kroemer. (2017).** Anticancer effects of the microbiome and its products. **VOLUME 15, AUGUST 2017.**
32. **Ahmed, H.Y.; Eissa, S.A.; Ghoneimy, E.A.; Ragab, A.M. and Sherif, M.M. (2008).** Characterization of [4{hex-l-Yen-3-ene),4(pent- 1,3-diene)l-amine; A Novel Hepatoma Growth-Inhibition Factor from Trichoderma viride. Sc J Az Med Fac (Girls); **29: l-17**
33. **Ahmed, H.Y.; Ghoneimy, E.A.; ElSheikh, H.H. and Elaasser, M.M. (2013).** Viability and cytotoxicity in tumor cell lines treated with fungal metabolites. ph.D. thesis. Botany and Microbiology Department Faculty of Science (Girls) Al-Azhar University.
34. **Abdel Aziz, A. K., Azab, S. S. E., Youssef, S. S., El Sayed, A. M., El Demerdash, E., & Shouman, S. (2015).** Modulation of imatinib cytotoxicity by selenite in HCT 116 colorectal cancer cells. Basic & clinical pharmacology & toxicology, **116(1), 37-46.**
35. **Ertmer, A., Huber, V., Gilch, S., Yoshimori, T., Erfle, V., Duyster, J., & Schätzl, H. M. (2007).** The anticancer drug imatinib induces cellular autophagy. Leukemia, **21(5), 936-942.**
36. **Kim, J. L., Lee, D. H., Jeong, S., Kim, B. R., Na, Y. J., Park, S. H., & Oh, S. C. (2019).** Imatinib-induced apoptosis of gastric cancer cells is mediated by endoplasmic reticulum stress. Oncology reports, **41(3), 1616-1626.**

37. **Attoub, S., Rivat, C., Rodrigues, S., Van Bocxlaer, S., Bedin, M., Bruyneel, E., & Gespach, C. (2002).** The c-kit tyrosine kinase inhibitor STI571 for colorectal cancer therapy. Cancer research, **62(17), 4879-4883.**
38. **Wu, Y. S., Ngai, S. C., Goh, B. H., Chan, K. G., Lee, L. H., & Chuah, L. H. (2017).** Anticancer activities of surfactin and potential application of nanotechnology assisted surfactin delivery. Frontiers in pharmacology, **8, 761.**
39. **Dey, G., Bharti, R., Dhanarajan, G., Das, S., Dey, K. K., Kumar, B. N., & Mandal, M. (2015).** Marine lipopeptide Iturin A inhibits Akt mediated GSK3β and FoxO3a signaling and triggers apoptosis in breast cancer. Scientific reports, **5(1), 1-14.**
40. **Zhao, H., Shao, D., Jiang, C., Shi, J., Li, Q., Huang, Q., & Jin, M. (2017).** Biological activity of lipopeptides from *Bacillus*. Applied microbiology and biotechnology, **101(15), 5951-5960.**
41. **Cao, X. H., Wang, A. H., Wang, C. L., Mao, D. Z., Lu, M. F., Cui, Y. Q., & Jiao, R. Z. (2010).** Surfactin induces apoptosis in human breast cancer MCF-7 cells through a ROS/JNK-mediated mitochondrial/caspase pathway. Chemico-biological interactions, **183(3), 357-362.**
42. **Yin, H., Guo, C., Wang, Y., Liu, D., Lv, Y., Lv, F., & Lu, Z. (2013).** Fengycin inhibits the growth of the human lung cancer cell line 95D through reactive oxygen species production and mitochondria-dependent apoptosis. Anti-cancer drugs, **24(6), 587-598.**
43. **Riera-Romo, M., Wilson-Savón, L., & Hernandez-Balmaseda, I. (2020).** Metabolites from marine microorganisms in cancer, immunity, and inflammation: A critical review. Journal of Pharmacy & Pharmacognosy Research, **8(5), 368-391.**